Characterisation of Cardiac Protein Changes Post Death: A Pilot Study.

Dissertation presented for the degree of Master of Science (Medicine)

by

Student: Dipolelo Mokaila (MKLDIP001)

Supervisor: Professor Ntobeko A.B Ntusi

Co-supervisor: Dr Evelyn Ngwa Lumngwena

: Professor L.J Martin

: Dr L Taylor

Word count: 15137

Dedication

I would like to dedicate this work to my parents, Ms Motjopi Stephina Mokaila and Mr Kgaogelo Madisha who have always been by my side throughout this journey. My grandmothers, Francina Mokaila and Mothepa Elizabeth Sete who raised me with love and respect. To my lovely brother, Molefi Desmond, my beautiful sister, Molemo Gaeonale, who have been my driving force to continue working hard. To all my baby cousins who still have a lot ahead of them. Lastly, I dedicate this to my gorgeous daughter, Dintle Linathi.

Declaration

I, *Dipolelo Mosebjadi Mokaila*, hereby declare that the work on which this dissertation/thesis is based is my original work (except where acknowledgements indicate otherwise) and that neither the whole work nor any part of it has been, is being, or is to be submitted for another degree in this or any other university. I empower the university to reproduce for the purpose of research either the whole or any portion of the contents in any manner whatsoever.

Signature: Signed by candidate

Date: 18/07/2024

Acknowledgement

- I would like to show gratitude and thank the following people:
- My supervisors, Prof. Ntobeko Ntusi, Dr Evelyn Lumngwena, Dr Laura Taylor and Prof. Lorna Martin, for the continued support, advice, and contribution on this project.
- Dr Royle for her contribution and training for sample collection.
- Mr Sango Skelem, thank you for being a brother during all those hectic autopsy early mornings.
- My colleagues who went out of their way to support and assist me when I encountered problems Dr Solomon Aremu, Mr Daniel Maitithu and Dr Carmelita Abrahams.
- To all CHI students and staff for all the teamwork and assistance at the office and making it a pleasant place to be.
- Prof. Zenda Woodman and Dr Bianca Abrahams, thank you for stepping in to assist me with lab work when I had lost hope, I really appreciate it.
- Salt River Mortuary staff for all the guidance, assistance, and laughter during those cold early mornings.
- To the families that that gave consent, I really cannot thank you enough, for this would not be possible without you; and may the souls of your loved ones continue to rest in eternal peace.
- My friend, Mushaisano Sivhaga, thank you for listening to all my complains and encouraging me to be strong.
- My spiritual pillars, TASA members for all the love and prayers
- To department of Medicine funding, VC scholarship and the National Research Foundation, thank you for affording me this enormous opportunity.

Table of Contents

Abstract

Background: Postmortem interval (PMI) is an important consideration in medicolegal death investigation. Methods such as temperature measurement, evaluation of muscle contraction, lividity, and decomposition rate are applied to estimate PMI, also referred to time since death. These methods are, however, affected by environmental factors that either delay or accelerate some of the processes. Expression, concentration, and stability of proteins do not remain the same after death. This varied behavior of proteins within the body has prompted numerous research approaches to characterise proteins to estimate PMI. It is through interaction of proteins with other micro-molecules that crucial signaling pathways and cellular processes are activated to drive mechanisms leading to health and disease of an organism. As a result, protein changes can be studied to gain insight into disease pathophysiology.

The evaluation the structural integrity of tissues from healthy individuals post death may provide a source of credible controls for research on biological samples harvested during surgery in individuals with known disease. It thus calls for the need to assess the biomolecule stability of such tissues when required as controls for studies.

Aim: To investigate how biochemical parameters change across brief PMIs for PMI estimation and subsequently to guide the selection of appropriate tissues as potential source of control samples for research.

Objective: To determine if there is degradation in cardiac proteins post death for bodies with known PMI to determine the usability of PM cardiac tissues as controls for research based on cardiac protein integrity over the PMI.

Methods: This was a cross-sectional, observational, quasi-experimental study. Changes in native vinculin, cardiac troponin cardiac troponin T (cTnT), cardiac troponin I (cTnI), and eukaryotic elongation factor (eEf1a) in cardiac tissues from decedents recruited at the Salt River Mortuary, Cape Town were evaluated using Western blotting (WB) assay. Image J analysis of protein intensities of native bands and degradative products were used to compare proteins from different PMIs (0 to 151 hours).

Results: We recruited and sampled 52 decedents**:** 30 individuals were sampled at PMI of greater than 72 hours, while 22 individuals were sampled at PMI of less than 72 hours. WB detection of 117 kDa vinculin protein showed this to be present in all left ventricular (LV) samples analysed. The degradation of this protein commenced at 37 hours and progressed with time in LV. In aortic valves (AV), vinculin was intact in tissues extracted from living individuals and cases with early PMI of less than 24 hours. Mitral valve vinculin was detected from 8-57 hours PM. cTnT obtained from the LV was present in all investigated cases. cTnT showed degradation bands in all cases with intensity increasing with time. cTnI detection in LV was present in majority of the cases during study period Lastly, we detected eEfa1 in all LV samples, and we found eEfa1 to be present in majority of cases and the band intensities also decreased with increasing PMI.

Conclusion: We aimed to understand biochemical changes that occur postmortem in cardiac tissues through analysis of biochemical molecules. While we observed changes in proteins in cardiac tissues with increasing postmortem intervals, our findings suggest that some cardiac proteins are stable during early time PMI and may be suitable to be used in PMI estimation. Additionally, we observed integrity of protein up to 72 hours PM, suggesting that cases sampled at that time may be suitable to be utilised as controls for research.

Abbreviations

ADAM9	A-disintegrin and a metalloprotease 9
ADD	Accumulated days degree.
ADP	Adenosine diphosphate
APS	Ammonium persulfate
ATP	Adenosine triphosphate
AV	Aortic valve
BCA	Bicinchoninic acid assay
BSA	Bovine serum albumin
CA	Coronary artery
CHI	Cape Heart Institute
CSF	Cerebrospinal fluid
cTnC	Cardiac troponin C
cTnI	Cardiac troponin I
cTnT	Cardiac troponin T
DNA	Deoxyribonuclease
ER	Endoplasmic reticulum.

eEfa1	Eukaryotic elongation factor 1
FasL	Fas ligand
G	gram
GAPDH	Glyceraldehyde 3-phosphate dehydrogenase
HAF	Hypoxia associated factor.
HPM	Hours postmorterm
Hx	Hypoxanthine
kDA	kilo Dalton
l	litre
LCE1C	Late conrnified envelope 1C
LPL	Lipoprotein
LV	Left ventricle/ventricular.
M6P	Mannose-6-phosphate
Min	Minutes
ml	Millilitres
mRNA	Messenger ribonucleic acid
MV	Mitral Valve

MW	Molecular weight
PAGE	Polyacrylamide gel electrophoresis
PH	Potential of hydrogen
PM	Postmorterm
PMI	Postmorterm Interval
PRKCG	Protein kinase C gamma
PTEN	Protein and tensin
SF	Synovial fluid
SRM	Salt River Mortuary
RNA	Ribonuclease
rpm	Revolution per minute
rRNA	Ribosomal ribonucleic acid
TBS-T	Tris-buffered saline tween
TEMED	Tetraethylediamine
TBS	Tris-buffered saline
TDS	Total decomposition score
tRNA	Transfer ribonucleic acid.
Ub	Ubiquitin
UCT	University of Cape Town
VH	Vitreous humor

℃	Degree Celsius

Introduction

Proteins are polymers made up of amino acid sequences synthesised in ribosomes and held together by peptide bonds. Proteins provide cellular support (in cytoskeleton and cell membranes), act as hormones, catalysts for cellular reactions, enzymes, and cell signaling molecules. They make up majority of the human organ systems, however, their expression varies from tissue to tissue, depending on the function and the state of the body [1]. These are regulated through processes such as protein synthesis, folding, conformational maintenance, and degradation to achieve homeostasis [2-4]. During postmortem, the expression, and stability of proteins do not remain the same, hence the investigation into the use of proteins during autopsy to estimate PMI [3, 4] [5] [6, 7].In 2017, Statistics South Africa reported 51 164 unnatural deaths and a rise of 1 415 in murder cases reported for 2022 compared to 2017 [8, 9], highlighting the necessity for development of reliable and efficient supplementary methods to estimate PMI to assist medicolegal investigations.

Several methods are utilised to estimate PMI, and these are based on decomposition, physiological, entomological, microbial, biochemical, and genetic changes[10-12]. Physiological changes such as body temperature changes, contractility of muscles and staining of the skin surface, respectively known as *algor*, *rigor* and *livor mortis* are some of conventional method used in estimation of early PMI. In some instances, muscle excitation following the application of external stimuli is used to estimate PMI. Physiological changes progress in a time-dependent manner allowing for correlation with PMI, however, they are effective in early PMI investigation [10, 11, 13, 14]. Additionally, entomology and body decomposition are utilised to estimate long PMIs, however, these methods are limited by variable geographical and climate conditions [12]. Consequently, PMI studies have shifted to using biological markers such as proteins to accurately estimate PMI. An added value is that these may inform the integrity of tissues in PM and their potential use as controls in scientific research.

Chapter 1

Literature Review

1.1 Protein degradation pathways

Protein degradation is a normal physiological process that maintains homeostasis to ensure proper functioning of the body and forms a vital part of our physiology by regulating protein concentrations and integrity [2]. Eukaryotic protein degradation is regulated through two major pathways: either by ubiquitination of proteins or lysosomal proteolysis pathway[15]. Ubiquitination entails the addition of ubiquitin (Ub) to a target protein. Ubiquitination controls the content of proteins within the body by making use of three enzymes to make the target protein identifiable for destruction. During the Ub molecule tagging, the carboxyl end of the Ub molecule is linked to nitrogen on the lysine amino acid of a target protein, forming an isopeptide bond, through hydrolysis of ATP. Ubiquitination is initiated by activation of the Ub molecule through E1 enzyme which acts as a transfer molecule. Enzyme cysteinyl residue on E2 then attaches to Ub on E1, leading to E1 dissociation. The E2 bound to the Ub molecule is then attached to the E3 enzyme, which acts as a mediator/ligase between the Ub and the target protein, this is a continuous process leading to polyubiquitination (Figure1). The polyubiquitinated of the protein molecule allows it to then attach to a proteosome complex for destruction. The 19s subunit of a proteosome complex unfolds the Ub-linked protein and attaches it to the 20s subunit, which contains the proteases that breakdown proteins into amino acid constituents [16].

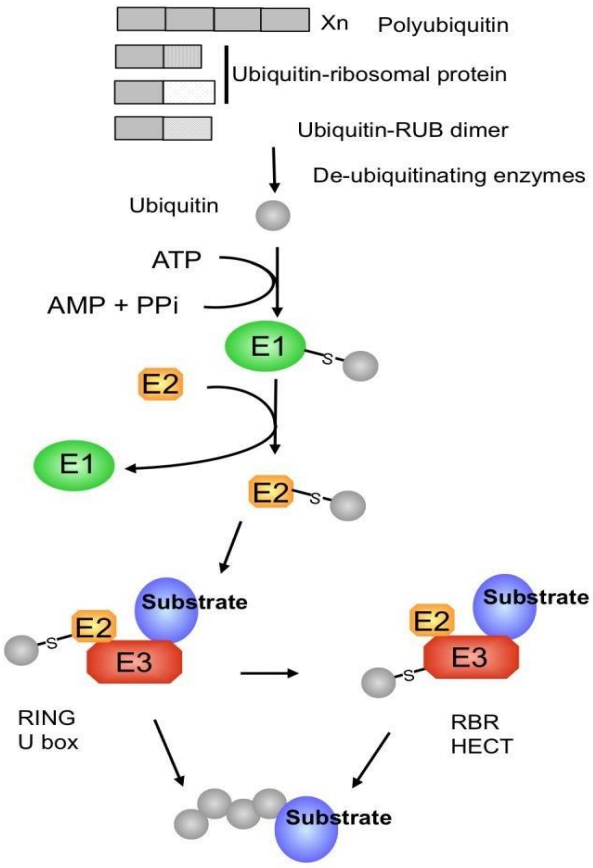

Figure 1: Ubiquitin genes and pathway. Callis, J., The ubiquitination machinery of the ubiquitin system. Arabidopsis Book, 2014. 12: p. e0174.

Lysosomes are membrane enclosed acidic organelles containing enzymes used to break down proteins [15, 17]. Lysosomes plays a crucial role in maintaining normal cellular metabolic activities, hence the regulator of homeostasis. An accumulation of proteins to toxic level causes disease. The lysosomal proteolysis pathway degrades large, long-lived, and damaged proteins instead of short-lived, misfolded proteins [18]. Lysosomal degradation either involves the endocytosis or autophagy pathways, both involving the internalisation of cellular constituents [17]. The endoplasmic reticulum (ER) synthesises lysosomal hydrolytic proteins that are in turn transported to the Golgi apparatus where they interact with the trans Golgi network (Figure 2). This interaction results in tagging of lysosomal proteins with mannose that becomes phosphorylated and forms mannose-6-phosphate (M6P) which later attaches to the M6P receptors on the Golgi apparatus and forms vesicle that burst from the Golgi apparatus. The vesicles containing lysosomal proteins then enters an acidic early endosome environment causing the release of M6P receptor from lysosomal hydrolytic proteins which interacts with target proteins contained in the endosome and results in protein breakdown (Figure 2) [17].

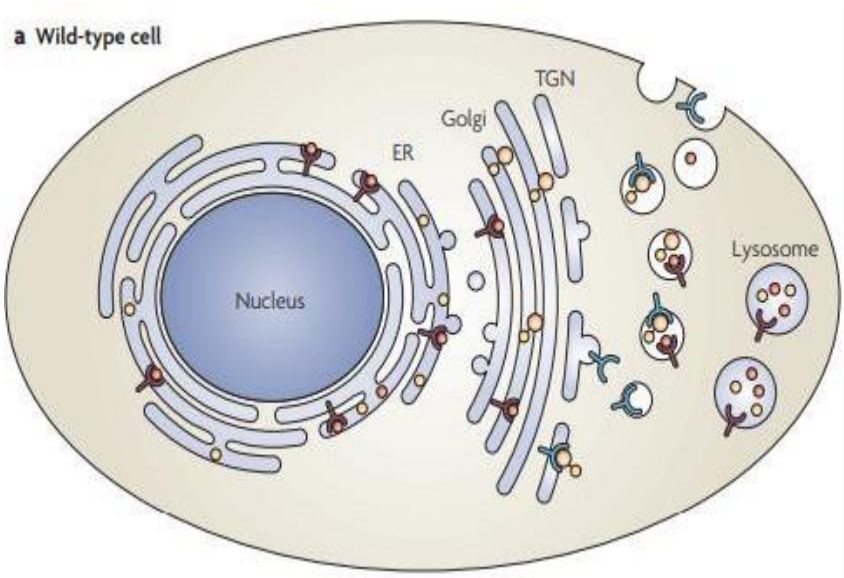

Figure 2: Lysosomal M6P receptor dependent pathway. Saftig, P. and J. Klumperman, Lysosome biogenesis and lysosomal membrane proteins: trafficking meets function. Nature Reviews Molecular Cell Biology, 2009. 10(9): p. 623-635.

1.2 The estimation of PMI with algor mortis

Algor mortis is used to refer to a decrease in normal temperature (37°C) following death to match the ambient temperature in a corpse environment [11]. Physiologically, the production of normal body temperature results from chemical energy obtained from food and mechanical energy from muscles and is regulated throughout the body by the hypothalamus via a process called thermoregulation [19]. Thermoregulation ceases after death, resulting in a declining body temperature [20]. The loss of heat occurs in timely manner, through conduction and convection, and can be used for estimation of PMI for up to 72 hours [10, 21].

Initially, estimation of PMI using temperature data only was believed to follow Newton's law of cooling, stating the rate of loss of heat from a surface of a solid body to the surrounding fluid is proportional to the difference in temperature between the surface and the fluid[22]. Subsequently, this hypothesis was debunked by Brown A, *et al* (1974) who stipulated a new law for objects having specific size and thermal properties [22, 23]. Additionally, the thumb rule, which states that for every 1hour passed, the body temperature decreases by 1°C, was disregarded since it did not stand up to experimental and epidemiological scrutiny [22-24]. Subsequently, different studies have derived mathematical models that estimate PMI using temperature data [22, 24]. Currently, the nomogram model developed by Henssge is frequently used to determine PMI [11, 25]. Unlike others, this method considers the type of coverings found on a body, levels of humidity, body mass, and requires a single rectal temperature measurement. Additionally,

temperature can be taken from axillary regions, inner ear, and nose [11, 25]. Although the method is in practice, factors such as cause of death and body mass index (BMI) continue to affect its accuracy [10].

1.3 Rigor mortis PMI estimation

Rigor mortis is described as the stiffening of body muscles following death [10]. During normal muscle contraction, calcium released from the sarcoplasmic reticulum binds to the troponin protein resulting in a structural conformation that exposes the myosin head [26]. Adenosine triphosphate (ATP) binds to the myosin domain and is hydrolysed to adenosine diphosphate (ADP), resulting in the formation of a cross bridge between actin and myosin, allowing muscle contraction to take place [26]. In the event of death, the body is not immediately deprived of ATP due to glycolytic processes that continue during early hours of death and cause muscle flaccidity. It is only when ATP levels drop to below 85% that muscles fail to relax, leaving muscles in the contracted state [14]. This process does not occur simultaneously in all body parts but progresses gradually starting in muscles of the heart and spreading in a successive manner from eyelids, neck, lower jaw, chest, upper limbs, abdomen, lower limbs, and then finally ending in the fingers and toes following Nysten's Law. The stiffening begins within an hour of death and is completed by 36 hours [10], implying that bodies achieve complete stiffening are over 36 hours after death. Forensic investigations make use of the position of the body in rigor and freeze expressions on the face to help in respective determination of whether the victim died in the place where the body was found and insights into the nature of death. However, muscle age and muscle mass may influence accuracy [11]. This method can only be used for PMI determination up to 72 hours. Besides its low sensitivity beyond 36 hours, the reliability of this method is affected by several other factors [10, 11].

1.4 Livor mortising estimating PMI.

Livor mortis, also known as hypostasis, is seen as blood staining on the skin surface of a cadaver. It results from the gravitational settling of the blood to the lower regions of the body. This occurs due the cessation of circulatory processes. It takes about 1 to 3 hours for this to be observed on a body and is completed in 6 to 8 hours [11]. In complete absence of oxygen in the body, *livor mortis* causes the body to stain blue and purple [26]. However, the use of stain colour to determine PMI stage does not provide adequate results since the type of staining is influenced by skin colour, intoxication state, blood haemoglobin level and body temperature during hypostasis [26, 27]. This method may assist in PMI estimation within 72 hours and it also provides evidence on whether the body was moved after death [27].

The response of skeletal muscle to external stimuli is divided into three phases, in the initial phase the entire muscle contracts when a force is applied to it, this is usually observed up to 2 hours postmortem. In the second phase, there is a formation of a strong reversible idiomuscular contraction pad that lasts for 5 hours postmortem and, finally a weak idiomuscular contraction pad develops and last for 12 hours postmortem[14]. Following the application of electrical stimuli, muscles contract strongly and successively spread to other neighbouring tissues away from the point of electrical application eventually causing complete muscle weakness. This procedure is usually done in orbicularis oculi muscles to easily observe the muscle movement. The manner in which contraction of orbicularis oculi muscle occurs is divided in to six stages to allow estimation of PMI (Table 1) [14].

Table 1. The degrees of response of orbicularis oculi muscle following electrical stimulation.

Muscle Contraction	**Time post-mortem (hours)**
1. Upper and lower eyelid + forehead + cheek	3.5 ± 2.5
2. Upper and lower eyelid + forehead	4.5 ± 2.5
3. Upper and lower eyelid	5.5 ± 2.5
4. Whole upper eyelid	8.25 ± 4.75
5. 1/3–2/3 upper eyelid	10.5 ± 5.5
6. Local upper eyelid	13.5 ± 8.5

1.5 Decomposition stages in estimating PMI.

Decomposition starts immediately after death and is completed by body skeletisation, initiated by the presence of bacteria and fungi which feed on the body causing the body to putrefy[30]. Purification is observed early in the abdominal area before spreading to the rest of the body[21].

The process of decomposition is divided into five stages that are correlative with PMI. These stages include (1) fresh, (2) bloated, (3) decay, (4) post-decay, and (5) skeletisation. The fresh stage is observed immediately after death with no gross decomposition observed. During the first stage of decomposition, changes such as cracking of the skin, development of greenish colour and *tache noir* [21, 30]. The development of green colour is mainly due to oxygen depletion and production of sulfhaemoglobin by bacteria in postmortem. This discoloration is usually first observed in the abdomen and may extend to the rest of the body as time progresses and insects are recruited to body openings and wounds [21].

The second stage of decomposition is characterised by bloating around the abdominal area and swelling in the eyelid area. The abdominal bloating is caused by gases produced from bacterial activities that take place in the abdomen during postmortem periods which additionally cause the temperature to rise in the body. During the decay stage of decomposition, there is evident gross putrefaction which comes as a result of insects scavenging on the body leading to skin breakages releasing gas and odour out of the body resulting from the expelled ammonium gas from the cadaver[21]. Insects such as

diptera larvae, *coleoptera*, *calliphoridae* and *sarcophagidae* are fully developed during this stage and their lifecycle can be used to deduce PMI [21, 30].

In post-decay stage, insects have eaten up most of body tissues leaving only pieces of skin and cartilage. This process continues until only bones are left and it is known as the skeletisation stage. However, before this stage, observable moulds begin to form on the surface of the skin[21, 30]. This formation of mould occurs due to inability of outer layer of the skin. In some cases, adiopocere formation takes place before complete skeletisation. In warmer conditions, this adipocere is not formed and the body goes directly into skeletisation[10]. Conditions such as air exposure, increased moisture, fungal growth, and the presence of Gram-positive bacteria promote formation of adiopocere[31]. The duration of each change is indicated in Table 2.

Overall, the rate at which decomposition occurs varies due to several contributing factors ranging from climatic condition, clothing, humidity and temperature, environmental pH, age, body treatment after death, extent, and type of injury to the individual, exposure to scavenging animals, burial type, and burial depth.[31].

In addition to qualitatively analysing the decomposed body to estimate PMI, other researchers have put forward quantitative methods by assigning body scores to the decomposed body [32]. These scores are attributed to different regions listed as face, neck, body and all the limbs. These regions are assigned individual scores ranging from zero (0) to six (6), with 0 indicating no changes and 6 complete skeletisations. The sum of each individual score is equal to the overall total decomposing score (TDS) (Appendix 1) [32, 33].

Accumulated degree days (ADD) is the average daily ambient temperature from the day of death to the day the body is discovered [34]. In 2013, Myburgh *et al*, used ADD and TDS to develop a mathematical model for estimating PMI. They discovered that since the decomposition process is affected by various factors such as climate conditions and inter-individual variations, the use of these type of models will only be applicable to certain groups and not in other and as a result yielding un-reproducible outcomes [32].

Table 2: Indications of decomposition changes at their corresponding time since death[21, 30].

Decomposition characteristics	Time since death
1. Greenish colour development	~2 days
2. Bloating	~3 to 14 days
3. Appearance of leathery skin	~10 to 30 days
4. Mould formation	~6 to 9 months
5. Skeletisation	≥1 month to 7years

1.6 Entomology in estimation of PMI

Postmortem entomology is focused on the identification of insects that are attracted to the decomposing body and study of their life cycle to estimate PMI. This method has been utilised for estimating of PMI in early and late postmortem periods [14, 35, 36]. When the body enters the putrefaction stage, several insects are attracted to the body by the smell. This recruitment and growth of insects is time-dependent, such that during the fresh stage no insect is found on the dead body unless in the presence of open wound on the body, causing premature colonization of insects and larvae formation [37].

The main insects studied include species of the order Diptera (flies) and Coleoptera (beetles). Their development is usually dependent on stage of decomposition [38]. Shrestha et al, (2020) reported that stage 3 and 4 of decomposition is associated with Hybotidae, Diptera and Fanniidae colonisation [10]. These insects utilise the decomposing body as the source of their nutrients and habitat for reproduction, therefore forensic entomology only allows the estimation of minimum PMI based on the age of insects [14]. The development of insect population is temperature dependent, and this should be taken in consideration when using entomology in estimating PMI [14, 36]. Thyssen et al, (2014) reported that tissue type plays a role in growth of insects [39]. Additionally, growth rate of insects is dependent on their sex, 10 times more growth in females as compared to males is reported [40]. Development of flies occurs faster at warm conditions as compared at cooler conditions and factors such as seasonality, toxins, and drugs and geographical areas can affect the development of insects [38]. Therefore, the use of entomology to estimate PMI needs to take several factors into consideration to allow for more precise estimation.

1.7 The use of microorganisms in estimating PMI.

The use of microorganisms in estimating PMI has also been of interest for researchers in Forensic Sciences. This was realised after the use of insects lifecycles in estimating PMI,

which may confer great inaccuracies [38, 41, 42]. When microbes such as fungi and bacteria use a dead body as their habitat and source of nutrients, they cause a change in the body pH and rupture of the skin and subsequent release of microbial products that get absorbed by the surface in contact with soil [30]. Following this process, the soil changes its pH and also the activity of microbes remaining within the body fluctuates. These processes occur in a time- dependent manner such that the quantification of microorganism is correlated with PMI [30, 42]. Examination of blood and cerebrospinal fluid (CSF) microbial community revealed that bacterial growth remained the same 48 hours in both compartments [43]. Studies on skin microbial community showed significant positive correlation with PMI [42]. A decrease in Bacteroides load is associated with an increasing PMI. The same was true for Lactobacillus while Bifidobacterium had no significant change. In all the investigated groups, the cause of death, sex, or weight had no influence on the relative abundance of microbes [44]. Liu, et al (2020) evaluated microbiome community in the brain, heart, and cecum for a period of 15 days. The results showed species such as Lactobacillus reuteri, Anaerosalibacter massiliensis, Proteus mirabilis and, Clostridium tetani E88 increase their abundance gradually up to 15 days. While the relative abundance of L. johnsonii decreased with increasing PMI also up to 15 days. Micro bacterium Enterococcus faecalis initially increased, then subsequently decreased in their colony [41]. This method exhibits potential to be used in conjunction with already existing methods for PMI estimation.

1.8 Estimating PMI using biological molecules.

The use of postmortem chemistry in forensic medicine emerged decades ago and is still an ongoing process whereby scientists are investigating its application in determining cause of death and estimating PMI [45]. The application of this method is based on the concept of autolysis and Fick's law of diffusion which describes the movement of particles from high concentration to lower concentration. It also makes use of the fact that metabolic processes do not come to a complete stop after death [46]. Scientists have therefore studied changes in electrolyte concentration in fluid compartments including CSF, pericardial fluid (PCF), vitreous humour (VH), synovial fluid (SF), and blood serum to estimate PMI [45, 47-52].

VH potassium (K+) concentration in cadavers has been correlated with PMI, and an increase in K+ concentration is associated with increasing PMI for periods within 100 hours [45]. In addition, aqueous humour, PCF, CSF, serum and SF K+ has shown positive correlation with PMI [45, 48, 49, 51, 53-57]. K+ concentrations in VH and CSF positively correlated with PMI while glucose, and sodium concentration in VH and CSF decreased with increased PMI. Strong correlation between PMI and glucose was reported in VH and Na+ concentration strongly correlated with PMI in CSF [58].

Ethnicity, alcohol, and hypoxanthine influence VH K+ [51, 61, 62, 63, 64]. Overall, VH serves as a good compartment when using analytes to estimate PMI over long periods since it is well protected from contaminants and autolysis occurs at a slower rate compared to other fluid compartments[59].

1.9 Leukocytes morphological changes in estimating PMI.

Morphological changes of leukocytes have been studied to estimate PMI. Changes were observed for up to 120 hours on a light microscope. The normal morphology of neutrophil, eosinophil and monocytes was maintained until 6 hours, with pyknosis and nuclear vacuolation observed at 12 hours, while nuclear disintegration was at 48-96 hours for neutrophils and at 48-72 hours for monocytes and eosinophils during postmortem period. The final morphological changes included the fragmentation of the entire cell. Neutrophil and eosinophil fragmentation was observed at 18 hours, followed by monocytes fragmentation at 24 hours. Lymphocyte pyknosis occurred at 36 hours, and nuclear disintegration at 96 hours, while fragmentation was observed at 72 hours. These time-dependent changes illustrated a significant correlation with PMI and could therefore serve as possible biomarkers for estimation of PMI [60]. Eosinophils and monocytes have been

reported to disintegrate at 144 hours, while lymphocytes degraded slowly for up to six days [61]. These findings imply that leukocyte changes are among the markers that could aid in late PMI estimation rather than in early stages of death.

1.10 Nucleic acid degradation in PMI estimation

Eukaryotic cells are comprised of deoxyribonucleic acid (DNA) and ribonucleic acid (RNA) which play crucial roles in organism functioning. DNA is double-stranded and a more stable form of nucleic acid than the single--stranded RNA. Other eukaryotic structures such as mitochondria contains a circular DNA compared to the rest of the cell, while RNA may exist in various forms inside cells including messenger RNA (mRNA), transfer RNA (tRNA) and ribosomal RNA (rRNA). The integrity of these nucleic acid in postmortem periods has been in question, and there is increasing research into their use in estimating PMI [62, 63].

1.11 DNA degradation and concentration in estimation of PMI

Numerous techniques have been employed in assessment of postmortem DNA degradation. These range from flow-cytometric analysis, polymerase chain reaction (PCR) and gel electrophoresis techniques. The use of flow-cytometric method to assess the splenic DNA content and its integrity in PM [62] revealed that the number of cells containing fragmented DNA increased with progressing PMI and fewer cells contained intact DNA[62] [63]. Several studies support the hypothesis that the rate of DNA degradation in an organ is dependent on the distance of the organ from the gut [64]. Late PMI estimation revealed that hepatic tissue is as a good candidate as compared to splenic tissue for this evaluation [64, 65].

1.12 RNA expression level and degradation level in estimation of PMI

Supplementary to DNA, the use of RNA as a tool for estimating PMI has also been evaluated. The majority of the studies focused on the mRNA expression levels and the evaluation of suitable tissue for PMI estimation [66-68]. An increase of total RNA degradation in blood and brain tissues has been observed with increasing time over 5 days PM [67]. The mRNA in the brain has been reported to change in a timely manner allowing for estimation of PMI in long PM period. Sex may influence the quantity of mRNA available in a tissue, with lower quantities reported in females relative to males. Additionally, age of death and blood pH affect the level of mRNA [69].

Expression of genes such as late cornified envelope 1C (LCE1C), hypoxia associated factor (HAF) and glyceraldehyde 3-phosphate dehydrogenase (GAPDH) has been investigated to estimate PMI [70-72]. LCE1C is a precursor of the cornified envelope, which plays a role in replacing keratin cell plasma membrane during differentiation [73]. HAF plays a key function in regulation of cellular response to hypoxia [74]. LCE1C has been studied for up to 5 days at differing temperatures of 25℃ and 40℃ and reported to have rapid decreased expression of the gene in low temperatures [73]. HAF has been studied in the brain for 48 hours PM with overexpression of this gene reported to be associated with increasing PMI [75]. GAPDH expression positively correlated with PMI in human brain tissue, however, this was influenced by gender and age, such that lower concentrations of mRNA were recorded in females relative to males, and high concentration recorded in older ages [69].

1.13 Proteomics in estimating PMI.

Protein such as vinculin, troponin T/I (TnT/TnI), eukaryotic elongation factor 1A (eEF1A) and tropomyosin (TPM) have been studied in PM for estimation of PMI [76-80]. These are cytoskeletal proteins that function in maintaining cell integrity. Vinculin is a 117 KDa protein that functions in linking talin to actin in the cytoskeleton and integrins in the cell [81]. Troponin is a regulatory protein that forms part of a ternary complex and assists in controlling calcium influx and mediation of actin to myosin interaction in muscle contraction [82, 83]. Vinculin and troponins degrade with progressed time in both skeletal and cardiac muscle and have been indicated as possible biomarkers for estimation of early PMI [82, 84]. For long PMI, TPM has been depicted as a suitable biomarker as it has been shown to maintain its stability for over 240 hpm.

Additionally, troponins degrade with progressing time during PM period. Cardiac Troponin T(cTnT) degrades as early as 34 hpm indicating that it can be utilised for early PMI estimation, however, degradation rate is affected by temperature with a rapid degradation observed at high temperatures [76, 77].

Other protein markers that have shown strong positive correlation with PMI in skeletal muscle include GAPDH and eEF1A for up to 96 hpm [78]. Talin 1 as a biomarker for PMI estimation has been demonstrated to positively correlate with PMI for up to 72 hpm, while cofilin and enolase have decreased expression with prolonged PMI [85, 86]. Apoptotic proteins such as fas ligand (FasL) and protein and tensin (PTEN) are good biomarkers for estimating early PMI of up to 6 hpm [87].

In summary, proteins have high resistance to time lapsed and adverse environmental factors as compared to other molecules and could potentially be evaluated as an additional method to aid in estimation of PMI [88]. We thus test the potential use of these proteins for PMI and aim to explore their useability as potential control tissues for studies that require make use of tissues that are hard to access in healthy human participants.

Chapter 2

Methods

This section outlines the study methods which include the design, sampling procedure, data collection, study site, and inclusion and exclusion criteria. It additionally, includes laboratory procedures for sample processing and detection of various proteins.

2.1 Study Aims and Objectives

2.1.1 Overall aim

To understand degradative changes that occur PM in cardiac tissues through analysis of the degradation of specific proteins over time.

2.1.2 Specific Objectives

To determine if there is degradation in cardiac proteins after death for bodies with known times since death.
To determine the usability of PM cardiac tissues as controls for research from cardiac protein integrity over time PM.

2.2 Study Design

This pilot study was a cross-sectional, observational, quasi-experimental study. The study investigated degradative changes in specific cardiac proteins in relation to PMI. Tissue biopsies were sampled from cadaveric hearts at the Forensic Pathology Services Salt River Mortuary (SRM) facility.

2.2 Study Area

Sample collection was conducted at SRM located in Salt River, Cape Town, Western Cape Province, South Africa. Sample processing was performed at the Cape Heart Institute (CHI), Faculty of Health Sciences, University of Cape Town (UCT).

2.3 Sampling

2.3.1 Study Population

This study required the use of heart tissues from cadavers; thus, the target study population were the deceased individuals whose forensic autopsies were conducted at the SRM during the sample collection period and whose families gave consent for participation in the study.

2.3.2 Inclusion Criteria

a. Deceased individuals between the ages of 18 and 80 years.

b. Deceased persons scheduled to undergo full autopsy examination at the SRM, whose families consented to participation in the study.

c. Individuals who died in hospital who have a known time of death, whose families consented to participation in the study.

2.3.3 Exclusion Criteria

a. Cases with history or/and macroscopic evidence of heart disease.

b. Cases with history or confirmed COVID-19 diagnosis at autopsy.

c. Cases where there was history or observation of sepsis at autopsy, cases of drowning and drug overdose.

d. Cases were excluded if the pathologist detected cardiac pathology at autopsy (see Table 3 below).

Table 3. Exclusion criteria

Evidence of previous cardiac surgery
A history of heart disease
Left ventricular hypertrophy (>15mm measured 2cm below the mitral valve)
Heart weight outside of these ranges*: MEN: 212 – 373g
WOMEN: 164 – 317g
Coronary artery (CA) atherosclerosis occluding >50% luminal surface area in right coronary artery left mainstem coronary artery, left anterior descending CA, or circumflex artery
Macroscopic previous myocardial infarction with area of fibrosis
Cardiac valve circumference outside of the reference ranges below**
Subjective thickening, calcification or fusion of valve cusps or chordae tendinae
Evidence of current or previous pericarditis (adhesions)
Suspected overdose

**[89, 90]

2.4 Ethical Considerations

2.4.1 Ethical Statement

The study was carried out in a manner that abided by the principles of the Helsinki Declaration. The Declaration states that: “In medical research involving human subjects capable of giving informed consent, each potential subject must be adequately informed of the aims, methods, sources of funding, any possible conflict-of-interest, institutional affiliations of the researcher, the anticipated benefits and potential risks of the study and the discomfort it may entail, post study provisions and any other relevant aspects of the study. The potential subject must be informed of the right to refuse to participate in the study or to withdraw consent to participate at any time without reprisal. Special attention should be given to the specific information needs of individual potential subjects as well as to the methods used to give the information”. Therefore, based on these principles, participation was voluntary, and participants’ families were not coerced into partaking in the study. They were also given an option to withdraw from the study at any time.

2.4.2 Approval

This is a sub-study (674/2020) to the main study both approved by the University of Cape Town Human Research Ethics Committee (HREC): 061/2018 and the Western Cape Provincial Government.

2.4.3 Informed Consent

The ethical and legal process based on the understanding that all medical activities should only be performed after a participant has been informed about the purpose, nature, consequences, and risks of the activity and has freely consented to it [91]. Informed consent was given by next of kin after thoroughly explaining the study to the families. Only cases whose families consented to taking part in the study were included.

2.5 Sampling Procedure

2.5.1 Consenting

Investigators went through consent training offered by the University of Cape Town’s Department of Forensic Medicine and Toxicology. The training entailed understanding the sensitivity of the study for the grieving families, how to handle the consent sessions, how to react in the event of unfortunate grieving behavior, and how to debrief. This was then followed by monitored consent sessions at the mortuary until the investigators were deemed competent to handle the consent sessions.

Next of kin were approached for consenting during the formal identification of their family member at the SRM facility. To ensure that families understood the information conveyed, consent sessions were carried out in a language that they were comfortable with, and they were allowed to ask questions during the session. In the event where the families could not understand or were feeling emotionally burdened, the consent session was stopped. Families that gave consent were then provided with the participant information sheet (PIS) containing information about the aims of the study, what is required from them and what samples (types, quantity) will be taken from their deceased relative. It also supplied contact details of the investigators and Chair of the Human Research Ethics Committee, should they decide to withdraw from the study or need further information at a later stage.

2.5.2 Sample Collection

The forensic pathology team was then notified of consented cases in order to get the autopsy date for sample collection. During autopsy, approximately 8*8*8mm sections of heart valves (aortic and mitral), left ventricle, and right atrium were extracted at room temperature by the forensic pathologist. The tissue sections were then collected into cryotubes, placed in ice (4˚C) for transportation to CHI and snap frozen in liquid nitrogen upon arrival before being further stored at -80˚C.

2.6 Sample Size

Consent sessions were held for 141 out of 396 cases identified from forensic records. 255 cases of these 396 were excluded due to autopsy before identification. 65 did not give consent and 22 cases were excluded at autopsy upon examination of the heart tissues, therefore 52 samples were collected and analysed.

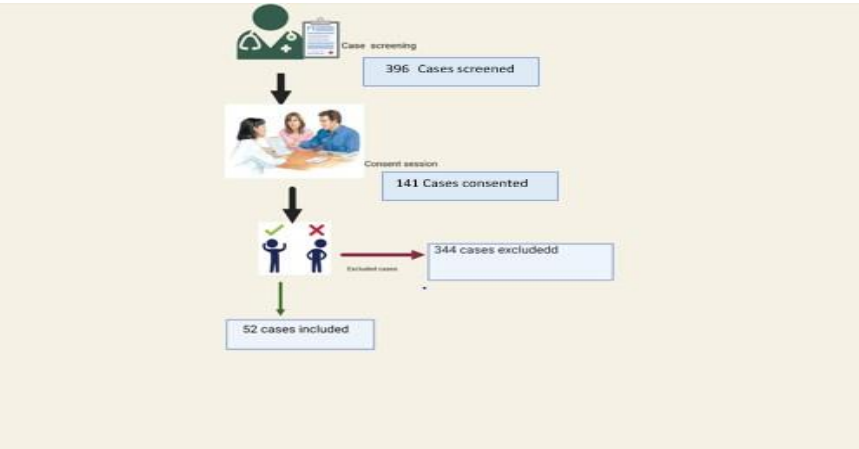

Figure 3: Recruitment process

The following text describes how the recruitment was done: Phase 1

During this phase, we recruited a pilot cohort (n = 22) whose PMIs were known and performed a preliminary assessment to determine whether cardiac proteins were degraded and the rate of degradation. These cases were in-hospital deaths which were referred to the SRM for determination of cause of death. Due to the nature of these cases, the PMI was short (less than 72hrs), which is a limitation for modelling PMI for this study.
A simple assessment to establish if there was protein degradation in the heart was performed. This addressed one of the fundamental objectives of this study, which was to assess the PMI period for which heart tissues of deceased individuals were still suitable for use as healthy controls in research studies.

Phase 2

This phase expanded the cohort (n = 30) to represent cases with longer PMIs (>72hrs). The motivation for this phase was to inform determination of time of death from cases with longer PMI.

2.7 Tissue Processing, Protein Extraction and Quantification

Tissues collected from the Forensic Pathology Services facility were snap frozen and stored at -80˚C until protein extraction. 40mg of snap frozen tissue was hammered and pulverised into fine particles under liquid nitrogen then added into Eppendorf tubes containing radioimmunoprecipitation assay (RIPA) buffer (50Mm Tris HCl, 150Mm NaCl, 0.5% (w/v) sodium deoxycholate, 1.0 Mm EDTA, 0.1 (w/v) SDS, 0.01 Triton X100, NaF, Na2VO3, and a protease inhibitor phenylmethylsulphonyl fluoride (PMSFO) dissolved in dimethyl sulfoxide (DMSO) (Sigma Aldrich. Merk, USA)). Samples were then sonicated for 1 minutes to complete homogenisation and incubated on ice for 1 hour while vortexing every 15 mins. They were subsequently centrifuged at 13,000 rpm for 30 minutes in a cooled centrifuge and supernatants were collected, protein quantity determined, and stored in single use aliquots at - 80˚c.

2.7.1 Protein Quantification

The bicinchoninic acid assay (BCA) principle states that a protein will interact with a cupric ion and convert it to a cuprous ion in an alkaline solution to form a cuprous complex. When a BCA molecule and this cuprous complex bind, a purple solution is

produced that absorbs light at a wavelength of 562 nm. The protein amount was then determined using the BCA kit in accordance with the manufacturer's instructions (Thermo-Fischer scientific, USA), by adding. 20 ul of protein extracts to 200 ul of BCA working reagent, which contained 50 parts of reagent A and 1 part of reagent B (Thermo-Fischer scientific, USA). Afterward, the solution was incubated for 30 minutes at 37oC, thereafter allowed to cool to room temperature, and then the absorbance was read using a GloMax® Multi Detection System.

2.8 Western Blotting

2.8.1 Sodium dodecyl sulphate polyacrylamide gel electrophoresis

Sodium dodecyl sulphate polyacrylamide gel electrophoresis (SDS-PAGE) was used to separate the proteins based on their size. We casted 7% stacking and 12% resolving gels (Appendices 3&4) for separation of GAPDH, B-actin, cTnT/I , Vinculin and eEf1A proteins. We then prepared 5x loading buffer containing bromophenol blue dye (Bio-Rad, CA,USA) to aid in tracking sample migration during electrophoresis (Appendix 5 for preparation procedure). Following this, 25% of B-mecarptoethathenol which is used as a reducing agent to break up disulphide bonds by cutting proteins to the right of the penultimate amino acids' carboxyl group (Sigma Aldrich. Merk, USA) was added to 75% of the 5x loading buffer to prepare the loading buffer for sample loading into the SDS electrophoretic gel. This reducing agent helped in linearising the protein before loading into the SDS gel wells. We then proceeded to add the loading buffer into an Eppendorf tube containing 20ug protein sample using 1:1 ratio. Afterwards, the sample was denatured at 95 °C for 5 minutes, allowed to cool and centrifuged to remove air bubbles before proceeding to add them into the wells using Hamilton pipette. 5 µl of protein ladder (Thermo- Fischer Scientific, USA) was loaded in to a separate well, casting trays with gel immersed inside the 1x running buffer(Running buffer: Tris, glycine and SDS (Sigma Aldrich. Merk, USA)) (Appendix 8 for preparation procedure) and gel was set run at 30 volts for the first 30 minutes and increased to constant voltage of 120 volts for 2 hours.

2.8.2 Blotting

After gel electrophoresis, immunoblotting was performed at 4°C at a current of 0.02A overnight in Towbin (transfer) buffer containing Tris base; glycine and methanol (Sigma Aldrich. Merk, USA) (Appendix 6) . Following the transfer, blocking buffer (5%Skimmed milk in 1X TBS-T) was used to block extra protein binding sites on the polyvinyidene

difluoride (PVDF) membrane (Thermo-Fischer scientific, USA) to prevent non-specific antibody binding for 1 hour (Appendix 7). The blocked PVDF membranes were then incubated with primary antibodies to our desired proteins. Mouse monoclonal anti-human GAPDH, B-actin , Vinculin ,cTnT/I and eEFa1(Santa Cruz Biotechnology Inc, CA, USA), diluted by 1:100 in 1XTBS-T buffer overnight at 4°C were used for primary detection of the proteins. Following primary antibody probing, the membrane was thoroughly washed 3times, each washing lasting for 10 mins with 1XTBS-T. This was followed by incubation with anti-mouse secondary antibody (Cell Signalling Technology, USA) diluted by 1:1000 in blocking buffer for 1 hour at room temperature. The secondary antibody probed membrane was then washed three times with 1XTBS-T, 15 mins for each wash cycle before membrane was ready for imaging to detect bound proteins.

2.8.3 Blot Imaging

To image the blots, 1:1 of chemilumiscent detection reagent 1 (stabilized peroxide solution) and chemilumiscent detection reagent 2 (enhancer solution) WesternBright™ ECL substrates were combined and poured over the membrane and incubated for 2 minutes following the manufacturer's instruction (Advansta Inc, CA, USA). The protein bands were then visualized by scanning using GeneSnap digital gel analysis system developed by Syngene. Membranes were stripped using a buffer (appendix 9) and probed with control antibody, GAPDH (Santa Cruz biotechnology Inc, CA, USA). For the depiction in the included figures, lanes were cropped, pasted, and adjusted for brightness and contrast.

2.8.4 Image J

To measure the relative amount of protein, Western blot bands were quantified by measuring the intensity of the native bands using ImageJ. The peak of each wave depicted the expression of a specified protein at each interval.

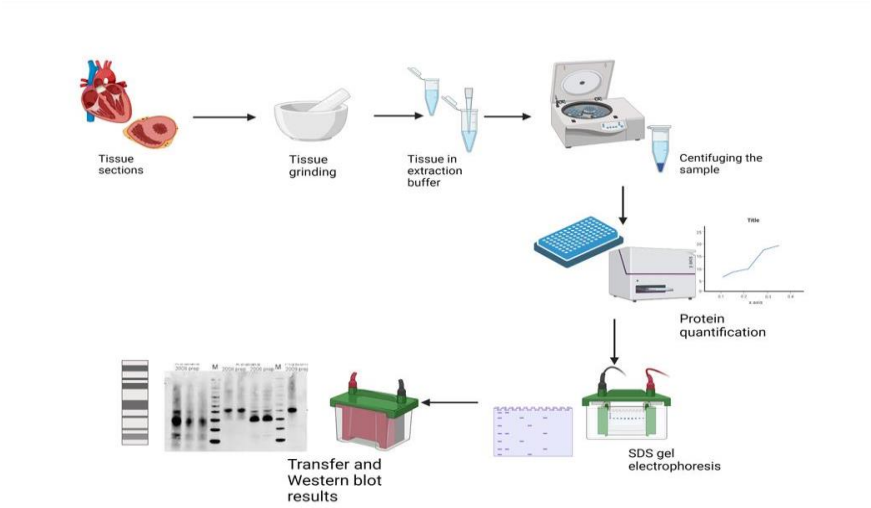

Figure 4:Experimental workflow for protein preparation

Chapter 2

Results

3.1 Recruitment and Collection

Fifty-two (52) cases were recruited: 22 cases autopsied less than 72 hours since demise; and 30 cases autopsied greater than 72 hours after demise.

Samples from included cases were sub-divided into sub-categories of time since death, for purposes of comparative analyses (Table 4).

Table 4: Western blot analysis

PMI groups	**0-24 hpm (N=1)**	**25-72 hpm (N=21)**	**73-120 hpm (N= 14)**	**121-145 hpm (N=8)**	**>145 hpm (N=8)**	**P-value**
Age (mean±SD)	43	41.7 ± 18.1	38.0 ± 17.7	34.0 ± 9.6	32.8±11.3	0.84

hpm = hours postmortem

3.2 Protein Quantification

We measured protein quantity using BCA assay in all included samples (19 in LV, 13 in AV and 12 in MV) with PMI ranging from 8hpm to 192hpm as indicated in the tables below.

Table 5: Left ventricle protein concentration

PMI (hpm)	Optical density	Estimated concentration as measured by BCA
8	0,990218	1885,974
32	0,982196	1799,201
37	0,998588	1981,089
46	0,976361	1738,699
49	0,9344326	1363,647
51	0,941011	1415,973
53	0,9094405	1184,8
55	0,9140766	1215,695
56	0,9222414	1272,581
57	0,979979	1775,954
61	1,000974	2009,073
61	0,9302759	1331,751
62	0,9248359	1291,336
70	0,9101868	1189,706
91	0,986442	1844,602
110	0,949191	1484,275
134	0,938605	1396,568
147	0,996673	1958,908
192	0,957875	1560,874

Table 6: Aortic protein concentration.

PMI (hrs)	Optical density	Estimated concentration as measured by BCA
0(BAV)	0,945265	1451,036
0(RHD)	0,95295	1516,904
0(RHD)	0,969997	1675,141
8	1,039602	2520,089
32	0,966779	1643,95
46	0,960533	1585,185
48	0,982929	1806,956
51	0,966501	1641,287
57	0,78648	659,6394
91	0,998298	1977,713
110	0,893506	1086,012
134	0,766729	614,4908
147	0,873	974,6003
192	0,882616	1024,748

Table 7: Mitral Valves protein concentration

PMI (hrs)	Optical density	Estimated concentration as measured by BCA
8	0,97422	1717,034
32	1,008511	2100,108
37	0,91739	1238,396
39	0,97298	1704,614
46	0,958157	1563,436
48	0,925438	1295,739
51	0,886737	1047,359
57	0,917251	1237,43
91	0,966533	1641,593
110	0,950942	1499,381
134	0,922838	1276,867
147	0,938272	1393,907

3.3 Protein Degradation in Tissues

3.3.1 Vinculin Protein in Left Ventricular (LV) Tissues

Vinculin is a 117 KDa cytoskeletal protein that functions as a major cell adhesion molecule, such that it attaches talin to actin in the cytoskeleton and integrins in the cell [81]. Vinculin is expressed ubiquitously including in the adrenal glands, appendix, bone marrow, brain, colon, duodenum, endometrium, oesophagus, gall bladder, heart, kidney, liver, lung, lymph node, ovary, pancreas, placenta, prostate, salivary gland, kidneys, small intestine, spleen, stomach, testes, thyroid, and urinary bladder[92].

Western blot analyses of LV tissues from samples with PMI from 8 – 192 hpm using anti-vinculin antibodies showed intact vinculin bands for all 11 biological samples with no degradative products.(bands) detected at 8 and 32 hpm samples (Figure 5.1a lanes 1 & 2). Two new low intensity and lower molecular bands, most probably representing degradation products of the 117 KDa protein were seen at ~100 and 95 KDa (degradation product (dp1) and degradation product (dp2), respectively). Degradation bands were detected from 46 until 192 hpm, except for the 110 hpm case where the intensity of these products was immensely low. The detection of internal control GAPDH indicated equal loading for all samples (Figure 5b).

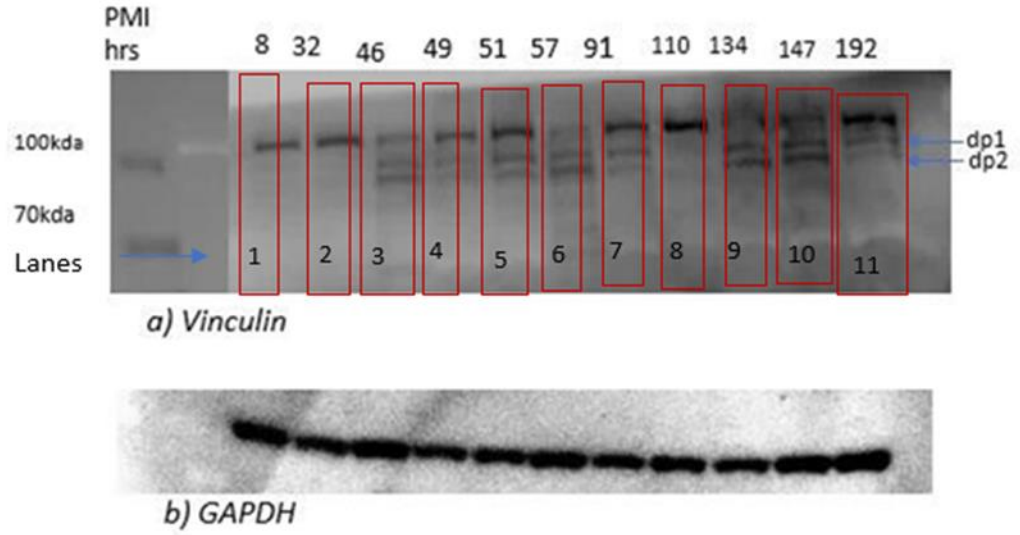

Figure 5: a) Degradative profiles of vinculin in LV tissues sampled at various times (8 hpm to 192 hpm) b) GAPDH used as internal loading control for all samples.

3.3.2 Vinculin Expression in Aortic Valves Post-Mortem

Similar to the LV tissue sections, we analysed 13 aortic valve (AV) tissue lysates from samples obtained at different times postmortem. In addition to tissues sampled from cadavers during forensic autopsy, we included three samples extracted from living individuals with cardiovascular complications at surgery. A native (intact) vinculin band (MW 117 KDa) was identified in all samples. As expected, there was no degradation for the first two samples from patients diagnosed with a bicuspid aortic valve (BAV) (living individuals), extracted during cardiothoracic surgery, labelled 0 hours (Figure 5.2a, lane 1 and 2). This was then followed by an appearance of 2 low intensity degradation bands of MW 70 KDa and 65 KDa on another 0- hour sample extracted from a patient diagnosed with rheumatic heart disease (RHD) (Figure 5.2, lane 3). This could possibly be due to tissue handling, storage, or protein sample contamination. At 8 and 32-hpm, vinculin appeared intact with very little to no degradation. Low intensity degradation bands with MW of 70 KDa and 65 KDa (dp1 and dp2, respectively) (Figure 5.2, lane 6-12) were seen for samples from 46 to 192 hpm. There was an appearance of an additional degradation band product (dp3) with MW of ~60 KDa for samples at 91 and 134 hpm (Figure 5.2, lane 10 & 12). An additional degradation band (dp4) appeared at 134 hpm but not at 147 hpm. These (dp4) protein products were no longer detected with anti- vinculin, probably due to degradation. The band intensities of the dp1, dp2 and dp3 were also reduced at 147 hpm likely due to degradation. Additionally, there was an appearance of a fourth degradation band (dp4) for samples at 134 hpm. B-actin (used as internal control) expression was detected; however, it was variable for all samples, indicating unequal sample loading.

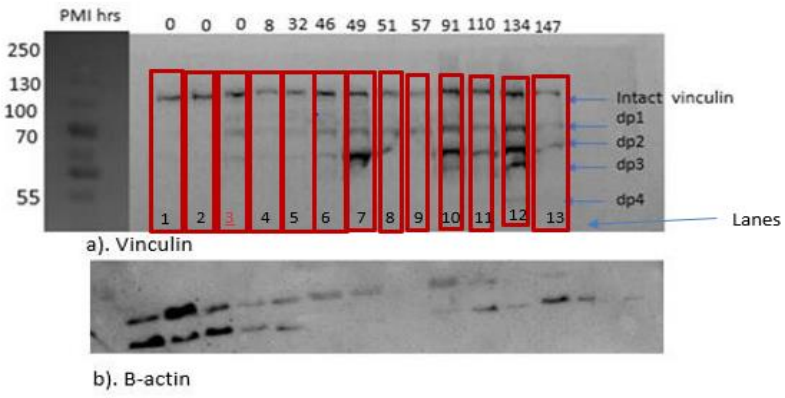

Figure 5.2: a) Degradative profiles vinculin in AV tissues sampled at various times postmortem 0 hours to 147 hpm; b) B actin which was used as internal loading control for all samples.

As beta-actin detection was not consistent across the lanes, despite our protein quantification and planned equal loading, we repeated the detection of vinculin in the AV, this time using GAPDH as loading control. Figure 5.2a confirmed the native or intact 117 KDA vinculin band in all our 13 investigated samples from 0 - 147 hpm. The first two 0-hour samples are those diagnosed with bicuspid aortic valve (BAV) (Figure 5.2a, lane 1 and 2) which showed an intact vinculin band with no degradation occurring. The third case at 0 hour was diagnosed with rhematic heart disease (RHD) and had an appearance of two low intensity degradation band products (dp1 and dp2) with MW of 70KDa and 55KDa, which could likely be due to poor sample handling. At 8 hpm, the 117 KDa protein remained mostly intact, with no or very low intensity degradation bands appearing at 55KDa for this case. From cases 32-147 hpm, low intensity protein degradation bands were evident at MW of 100 KDa, 70 KDa and 55 KDa (dp1, dp2 and dp3, respectively – Figure 5.3, lane 5-12). At 134 hpm, there was an appearance of an additional degradation (dp4) band at MW of ~50KDa, which was not evident in the 147 hpm sample, probably due to degradation. The GAPDH (MW 36 KDa) control used as an internal loading control was more consistent with the intensities of the vinculin protein bands than B-actin.

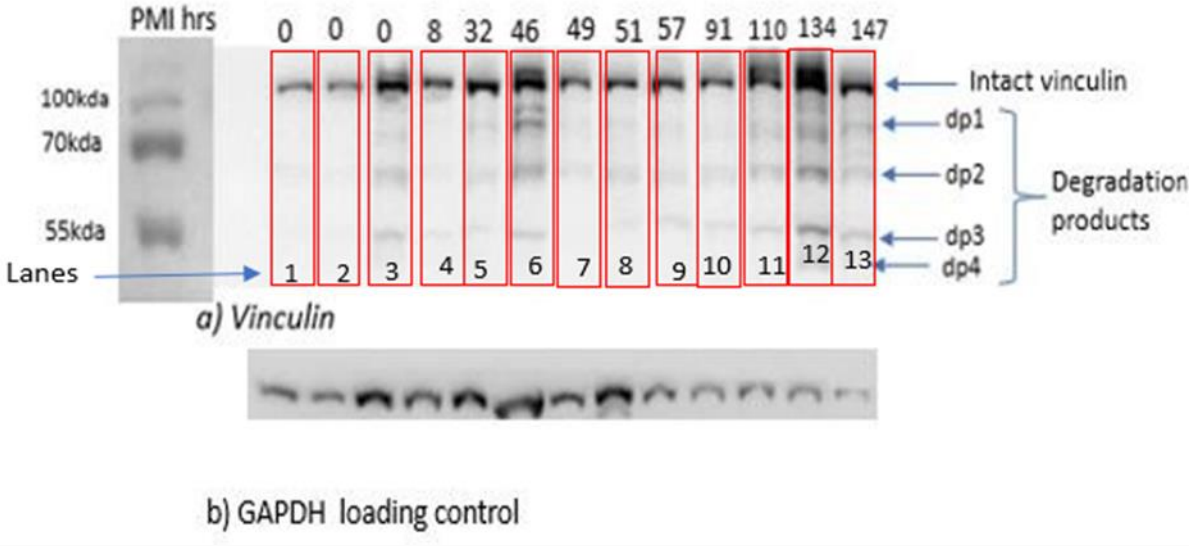

Figure 5.3 a) Western blot (WB) indicating degradative profiles of vinculin protein in AV tissues sampled at various times 0 hours to 147 hpm; b) GAPDH used as internal loading control for all samples.

3.3.3 Vinculin Degradation in Mitral Valve

The mitral valve (MV) is found between the LV and left atrium (LA) of the heart, enabling normal (forward) blood flow from the LA to the LV during diastole, while preventing blood backflow from the LV to the LA during systole [93]. At 8-57 hpm, there was a detection of native intact bands of 117 KDa cytoskeletal vinculin protein in the MV with appearance of intact bands and no evidence of degradation in this blot. An appearance of double bands (150 KDa and 117 KDa) at 48 , 51 and 57 hpm was noted; this may be attributed to vinculin isoforms known as meta-vinculin (Figure 5.4, lanes 6,7 & 8). Some studies have found co- expression of meta-vinculin and vinculin in cardiac and smooth muscles from the 91 hpm samples onwards. The detected protein bands became faint and almost undetectable in the 134 hpm case, suggesting degradation of the protein. From this Western blot, there was an onset of MV vinculin degradation evident after 46 hpm. Evidently, there were no detectable degradation products of vinculin in the MV tissue of samples we assayed. After stripping PDVF membrane and probed with GAPDH, however there was no detection. The absence of GAPDH could be results of membrane stripping that tends to diminish the detection signal or unsuccessful membrane stripping due to limited incubation period.

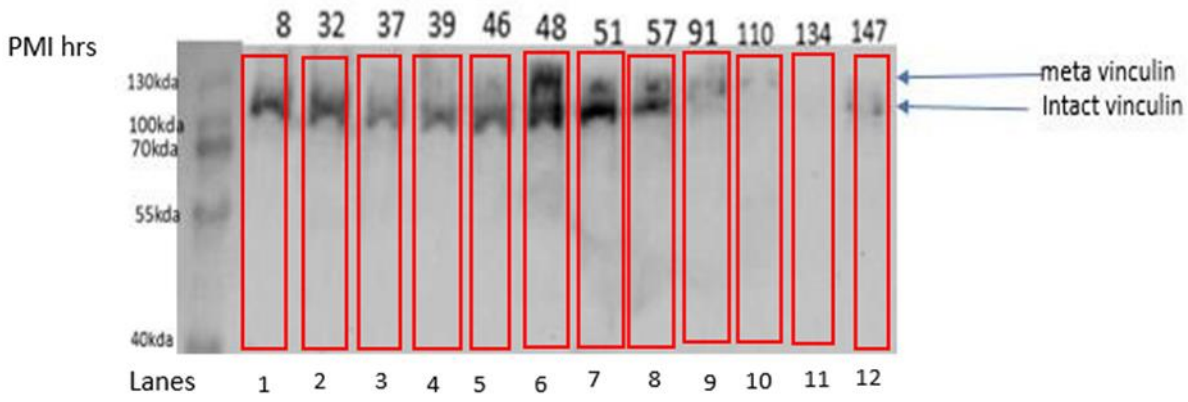

Figure 5.4: Degradative profile (Western blot (WB) of vinculin protein in MV tissues sampled at various times postmortem from 8 hpm to 147 hpm.

3.3.4 Comparison of vinculin degradation between early to late PMI in LV tissues for determination of time since death

PMI determination is important in forensic casework, at least for the determination of when a victim demised. As most of the proteins' degradative bands occurred relatively early, it was investigated whether appearance or disappearance of specific degradative

bands can differentiate early from late PMI.

LV tissue biopsies sampled before 72 hpm were analysed together and the degradation pattern of vinculin was compared to tissues sampled after 72hpm. There was a detection of intact native vinculin protein in all samples with less than 72 hpm (Figure 5.5) with apparent absence of degradation only in the 8 hpm sample. The intensities of the native bands were high for samples at 55, 56, 61, 62 and 70 hpm (Figure 5.5, lanes 7-9 & 11-12) compared to the rest of the samples. At 8 hpm this protein did not show any degradation. It was only at 37 hpm where this protein started degrading, shown by the appearance of two low intensity bands with MW of ~70 KDa and 60 KDa (Figure 5.5, lanes 2-12). An appearance of additional faint band of 55 KDa at 49, 51 and 61 hpm (Figure 5.5, lanes 4, 5 & 10). We could not detect GAPDH for this blot and this could be as a result membrane stripping that tend to decrease of robustness of second signal. The other reason for undetectable bands could be low antibody concentration.

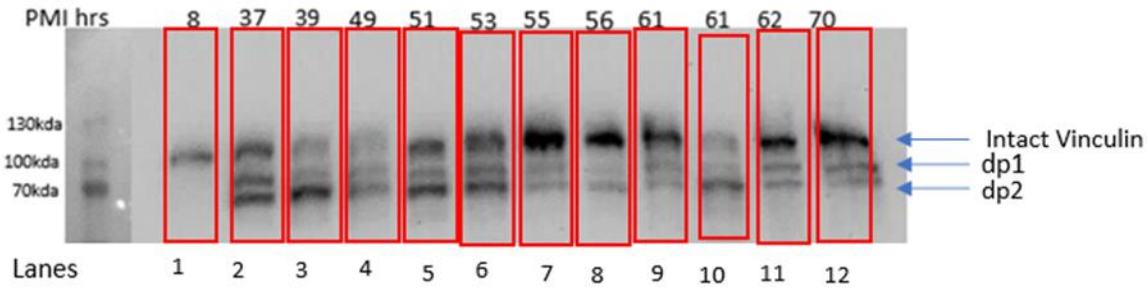

Figure 5.5: Western blot (WB) of vinculin protein in LV tissues sampled at various times post- mortem from 8 hours postmortem to 70 hpm.

3.3.5 Detection of Degradation Profiles of Cardiac Troponin T and I (cTnT/TnI) proteins in cardiac biopsies with increasing PMI

Cardiac troponin T (cTnT) and troponin I (cTnI) are cardiac regulatory proteins that regulate calcium mediated interaction between two cardiac proteins, actin, and myosin, controlling contraction of skeletal and cardiac muscles [94]. These proteins are expressed predominantly in the myocardium [95, 96]. There are 3 isoforms of cTnT found in the normal heart; the hcTnT1 and hcTnT2 isoforms are expressed in the foetal heart and hcTnT3 isoform is found in adults [97]. cTnI is the primary isoform expressed in adult hearts while foetal human heart expresses the slow-twitch skeletal Troponin I (ssTnI) isoform [98].

cTnT detection in LV

When the antibody to the 39 KDa cTnT was used to probe LV tissue lysates of biopsies sampled from PMI 8 – 192 hpm, we observed the full intact protein from 8 hpm to 192 hpm (Figure 5.6a), although very faint in the 48 and 57 hpm samples. We observed a lot of variability in the intensity of the protein bands from 37, 39, 48, 57 and 192 hpm. The full intact protein was slightly lower in intensity than the other bands, which was not evident in the GAPDH loading control. There was also an appearance a faint 36 KDa degradation band (dp1) which was faint at 8 hpm but increased slightly over time in the samples with increased PMI, while disappearing again at 192 hpm (Figure 5.6). The second degradation product (dp2) with MW of ~20 KDa was also very faint at 8 hpm but increased with increasing PMI time until 147 hpm; and was apparently broken down further as shown by the disappearance of this band at 192 hpm (Figure 5.6, lane 6 & 8).

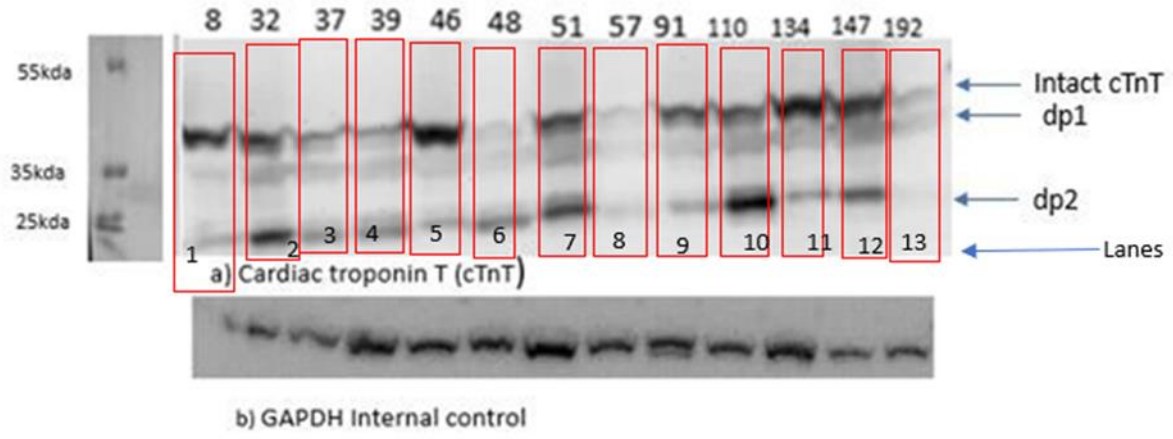

Figure 5.6: a) Western blot (WB) of cTnT protein in LV tissues sampled at various times (8 hpm to 192 hpm); b) GAPDH which used as internal loading control for all samples.

3.3.6 Cardiac Troponin I Detection in LV

The detection of 28KDa cTnI in 12 LV tissues showed the presence of intact bands in majority of the samples with no additional bands for degradation products observed. However, the intensity of the bands was high at early hours up to 91 hpm, and decreased with increasing PMI which was confirmed by ImageJ analyses of the protein bands (Figure 5.7c). There was however absence of this protein at 48 and 57 hpm this could be result of improper sample handling and storage that lead to complete degradation (Figure 5.7a, lanes 5 & 7). The overall trend seen is a reduction in the intensity of the protein from 46 hpm, and an even a greater reduction from 110 hpm onwards, suggesting degradation of the native whole protein. However, due to the very low molecular weight of cTnI and

the 12% acrylamide gels used, the detection of lower molecular weight degradation products could not be detected.

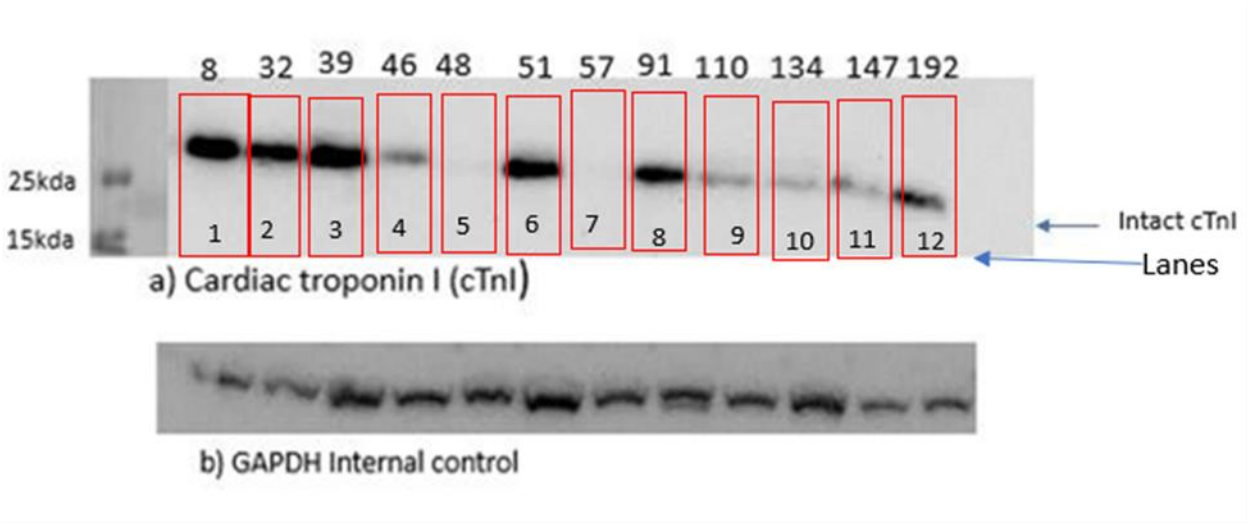

Figure 5.7: a) Western blot (WB) profiles of cTnI protein in LV tissues sampled at various times (8 hpm to 192 hpm) b) GAPDH which used as internal loading control for all samples.

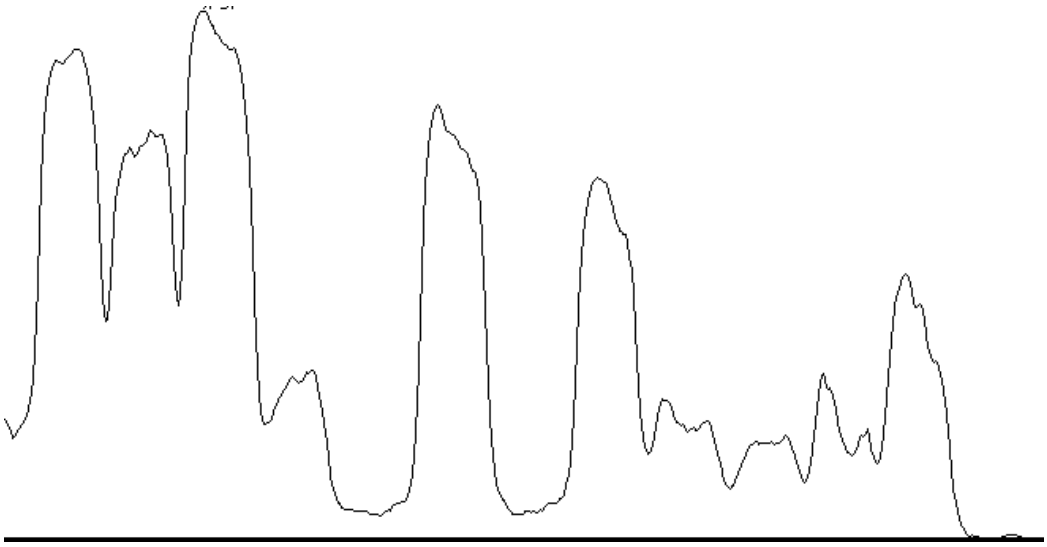

Figure 5.7: c) Image J analyses showing cTnI profile with increasing time.

Detection of degradation of eukaryotic translation elongation factor 1A (eEF1A) protein in cardiac biopsies with increasing PMI.

Eukaryotic translation elongation factor 1A (eEF1A) is a protein that is responsible for transporting aminoacyl-tRNAs (aa-tRNAs) to the ribosomal A-site and enables appropriate codon-anticodon-mediated translation of the genetic code [99]. This protein has been reported to degrade with increasing time in postmortem and suggested as a possibly suitable protein for estimation of PMI in a previous study in animals[100].

The detection of eEF1A with MW of 50KDa in LV depicted the presence of native protein

in all samples. A high intensity band was detected at early PMI of 8 hpm, and a decreasing pattern seen in the subsequent samples with time seen until 192 hpm (Figure 5.8a) which had a faint band despite the stability of the loading control (Figure 5.8b) suggesting degradation. A rapid decrease in intensity of bands at 48 and 57 hpm was also seen in cTnT probably due to inappropriate handling of those two samples at the mortuary or samples at the laboratory. As the degradation products were too small to detect on this Western blot, ImageJ plot comparison of the intensities of the intact eEF1A which visually showed decrease, confirmed this decrease with intensity as PMI increased (Figure 5.8c). The detection of GAPDH also indicated equal loading (Figure 5.8b).

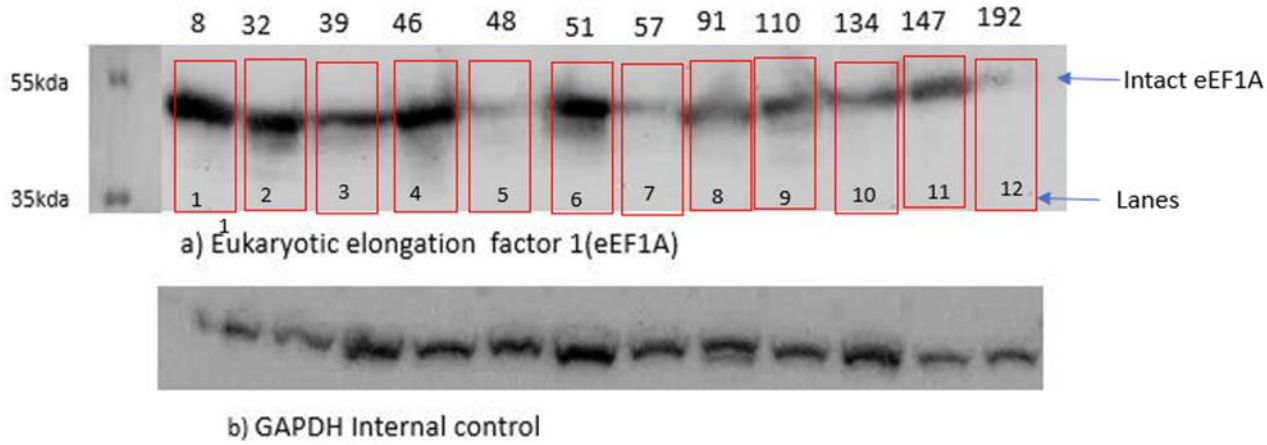

Figure 5.8: a) Western blot (WB) of eEF1A protein in LV tissues sampled at various times postmortem 8 hpm to 192 hpm; b) GAPDH used as internal loading control for all samples.

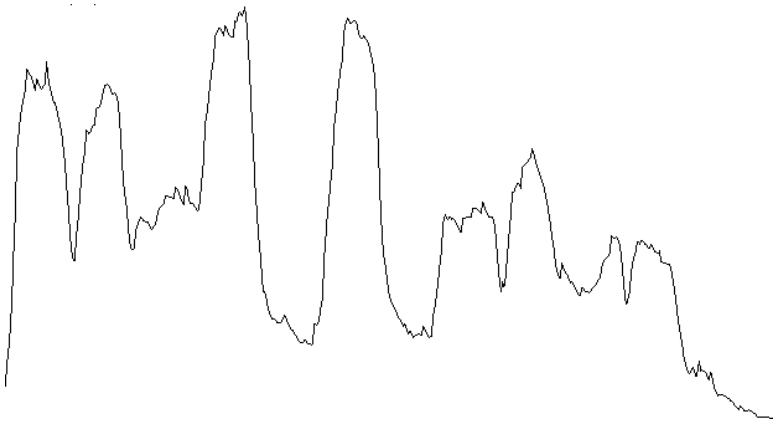

Figure 5.8: c) ImageJ profile of the changes in eEF1A proteins over PMI.

In summary, protein detection in cardiac tissues indicated that protein degradation occurs in a timely manner, remaining stable at early PM hours and degrading later. Vinculin protein appeared, in this study, to be a more suitable protein to be used as biomarker for PMI estimation in early hours rather than cardiac troponins that tend to remain stable for

long and may be useful for PMI estimation of longer duration.

Chapter 4

4.1 Discussion

Characterisation of protein degradation in postmortem cases is an essential test that may aid in forensic medicolegal investigations. It is crucial to identify suitable proteins for PMI estimation to enable informed recommendations and conclusions. For this study, we selected cardiac proteins that have been reported to degrade with progressing time in postmortem period to investigate the utility of these proteins as biomarkers for estimating PMI. The choice of cardiac tissues was also to guide future research on use of cadaveric tissue as controls for research, especially by our current research project using cardiac tissues to understand the pathogenesis of rheumatic heart disease. Our current study has evaluated the degradation of these cardiac structural proteins for PMI determination.

4.2 Vinculin PostMortem Degradation

Vinculin (MW 117kda) is a cytoskeletal cell adhesion protein that attaches to surface of the cell through phospholipids [81]. This protein has no enzymatic activity and relies on protein- protein interaction for its functioning [101]. A study conducted by Pittner, et al (2020) using human samples demonstrated that this protein degrades at a rapid rate in cardiac muscles compared to skeletal muscles after death[84]. Another study showed that vinculin remained intact for 72 hpm [2]. That this protein remains intact for prolonged periods in cardiac tissues during the postmortem period has been supported by Tomita, et al (2004) who investigated changes in the kidneys, liver, cardiac and skeletal tissues, demonstrating that skeletal muscle has delayed postmortem changes compared to cardiac tissue [102]. Our data corroborates prior studies, demonstrating vinculin to be intact up to 32 hpm, with degradation starting at 37 hours and progressing with time in LV tissue.

Notably, vinculin remained intact in mitral valve tissue with no visible signs of complete degradation of the full-length protein by molecular weight shift, however, we observed a decrease in band intensity as time progressed. Intramuscular variation in vinculin degradation has been reported in the study conducted by Pittner et al (2020) [84]. We noted that myocardium expresses early signs of decomposition compared to valves and this may explain the increased degradation of proteins in certain muscle tissues. The other probable reason for variation in degradation pattern may be due to differences in rates of tissue decomposition for tissue components such as myocardial fibers, connective tissue,

and the vascular system [103].

The exceptional detection of vinculin in a case at 110hpm in LV with no signs of degradation may be related to how the body was stored (earlier refrigeration) in comparison with other cases where degradation was observed. Another reason for the variability in 110hmp could be attributed to epigenetic variation among deceased individuals. In our additional aortic valve experimental findings, we found vinculin to be intact for samples at 0-hours (living controls) and 8 hpm and that vinculin started degrading from samples 32-147 hpm. These findings confirm those of Zissler, et al (2018) who depicted the degradation of vinculin after 24 hours of death [104]. Vinculin seems to be a suitable biomarker for estimation of PMI since it degrades with time and may inform pathologists and other researchers that tissues at 8 hpm can be utilised as controls.

4.3 Cardiac Troponin(s) PostMortem Degradation

Cardiac troponins are regulatory proteins that are found within heart muscles and are bound by calcium during contraction, resulting in structural conformation that allows for interaction of myosin and actin filaments. These troponins exist in three forms: cardiac troponin T(cTnT), cardiac troponin C (cTnC) and cardiac troponin I (cTnI) and have been used as diagnostic markers for acute myocardial infarction post death, and additionally as a marker for the estimation of PMI [76, 105, 106].

To characterise cTnT degradation with time, Kumar, et al (2016) evaluated human cadaveric samples with varying PMI and found that degradation commenced as early as 5 hours after death, and progressed with time; however, degradation seemed to vary with the cause of death [107]. In another study, Kumar,et al (2016) investigated the dependency of cTnT degradation on temperature and demonstrated that cTnT remains intact during the early hours of the postmortem period, and at lower temperatures, while drastic degradation occurs at higher temperatures.

We did not evaluate the effect of cause of death and temperature on cTnT protein degradation. We controlled for temperature by making sure we worked on cases and samples stored at the same temperature pre- and post-extraction. One study reported cTnT remains stable for up to34 hours postmortem [77]. This finding was consistent with our observations of cTnT remaining intact for 8 hpm with degradation commencing at 32 hpm in the LV. The degradation bands decreased intensity as time increased, proving the possible utility of this protein in early PMI estimation.

Limited research studies have looked at cTnI degradation post death. cTnI has been found to remain intact within 24 hours and to start degrading afterwards in cardiac muscle [82]. In contradistinction, we found cTnI to remain intact over 10 days with varying expressions, such that it is highly expressed in early postmortem and less expressed in late PMI. This degradation of troponin is driven by activity of calpains and cathepsin that are highly activated and expressed in the post-mortem period [108, 109].

4.5 Eukaryotic Translation Elongation Factor 1A Degradation in PostMortem

Eukaryotic translation elongation factor 1A (eEF1A) is an actin binding protein that plays a role in the formation of filamentous actin (F-actin) bundles which function in the formation of cytoskeletal, cell cortex and stress fibers in mammals and regulate the shape and mobility of cells [110, 111]. This protein additionally recruits aminoacyl t-RNA to the ribosome and moves the elongating polypeptide from the ribosomal A site to the P site during translation [112].

eEF1A exists in two isoforms, the eEF1A1 and eEF1A2. In 2009, Kyoung-Min Choi and colleagues undertook a study to identify suitable biomarkers to be used in PMI estimation using rats and mice for biomarker identification and reported glyceraldehyde 3-phosphate dehydrogenase (GAPDH) and eEF1A2 to consistently decrease with increasing PMI when investigated for 96 hpm [100]. We investigated eEF1A for over 10 days in the LV and found this that band intensity decreased with increasing time, however, no degradations bands were detected. Our results differed from what has been reported by Kyoung-Min Choi et al, likely due to the fact that the detected eEF1A1 isoform is mainly expressed in the brain, placenta, lung, liver, kidney, and pancreas while the heart, and skeletal muscle expresses eEF1A2 isoform [92].

The detection of B-actin as an internal control showed variable expression on all our cases. This variability in expression has been reported in several studies and has been shown to be associated with the tissue hypoxic state following death through transcriptional activation of B-actin by nuclear respiratory factor-1[113, 114]. This then led to the switch to using GAPDH as loading control in our subsequent experiment. GAPDH has been widely used as loading control used in comparison of gene expression due to its consistent expression in tissues at different times [115, 116]. This ability to remain consistent has been shown in our study findings thus allowing to read the different expression level of proteins between cases at different PMI.

4.6 Conclusion

We aimed to understand protein changes that occur postmortem in cardiac tissues through analysis of specific proteins degradation changes. Our results showed evidence of vinculin, troponin and eEF1A protein degradation post death in cardiac tissues. These proteins have demonstrated their ability to retain stability in early postmortem (<24 hpm) with degradation commencing at around 37 hpm thus support their utility as biomarkers for PMI estimation in both early and long periods.

4.7 Limitations

SRM performs 4000 autopsies a year for the purpose of determining the cause of death, nature, and extent of underlying natural disease, and to enable learning, teaching, and research [117]. We had difficulty in obtaining enough cases with PMI of less than 24 hpm. These challenges were due to the following:

- Stringent inclusion and exclusion criteria such that only hospital cases were included.
- Scheduling of autopsies later than 24 hours due to increased backlog at the SRM.
- Swopping of autopsy slots leading to delayed postmortem examination for our consented cases.
- Delayed case identification by families / relatives.
- Consent refusal and withdrawals due to religious and cultural beliefs.

We were, however, able to demonstrate degradation in some of our experiments, supporting the use of these proteins as PMI biomarkers.

References

1. LaPelusa, A. and R. Kaushik, *Physiology, Proteins*, in *StatPearls*. 2022, StatPearls Publishing Copyright © 2022, StatPearls Publishing LLC.: Treasure Island (FL).
2. Klaips, C.L., G.G. Jayaraj, and F.U. Hartl, *Pathways of cellular proteostasis in aging and disease.* J Cell Biol, 2018. **217**(1): p. 51-63.
3. Paltian, J.J., et al., *Post-mortem interval estimative through determination of catalase and Delta-aminolevulinate dehydratase activities in hepatic, renal, skeletal muscle, and cerebral tissues of Swiss mice.* Biomarkers, 2019. **24**(5): p. 478-483.
4. Dasgupta, S.M., et al., *DETERMINATION OF POSTMORTEM INTERVAL BY TOTAL PROTEIN ESTIMATION AND ELECTROPHORETIC ANALYSIS OF SERUM-PROTEIN.* Journal of the Forensic Science Society, 1984. **24**(4): p. 301-301.
5. Fernandez-Rodriguez, A., et al., *Post-mortem microbiology in sudden death: sampling protocols proposed in different clinical settings.* Clin Microbiol Infect, 2019. **25**(5): p. 570-579.
6. Yadav, A., et al., *Determination of postmortem interval by decomposition changes: An ambiguous phenomenon.* Clinical Case Reports and Reviews, 2017. **3**.
7. 2002., T.i.c.a.g.o.o.t.g.b.o.i.G.W., *<924156220X.pdf>.* (2002).
8. Africa: M.a.c.o.d.i.S. and F.f.d. notification, *<P030932017.pdf>.*
9. *<fourth_quarter_presentation_2021_2022 (1).pdf>.*
10. Shrestha, R., T. Kanchan, and K. Krishan, *Methods of Estimation of Time Since Death*, in *StatPearls*. 2020, StatPearls Publishing StatPearls Publishing LLC.: Treasure Island (FL).
11. Shedge, R., et al., *Postmortem Changes*, in *StatPearls*. 2020, StatPearls Publishing StatPearls Publishing LLC.: Treasure Island (FL).

12. Amendt, J., et al., *Forensic entomology: Applications and limitations.* Forensic Science, Medicine, and Pathology, 2011. **7**(4): p. 379-392.
13. Mathur, A. and Y.K. Agrawal, *an overview of methods used for estimation of time since death.* Australian Journal of Forensic Sciences, 2011. **43**(4): p. 275-285.
14. Madea, B., et al., *Postmortem Changes and Time Since Death*, in *Handbook of Forensic Medicine*. 2014. p. 75-133.
15. Ray, S., *The Cell: A Molecular Approach.* Yale J Biol Med, 2014. **87**(4): p. 603-4.
16. Callis, J., *The ubiquitination machinery of the ubiquitin system.* Arabidopsis Book, 2014.**12**: p. e0174.
17. Saftig, P. and J. Klumperman, *Lysosome biogenesis and lysosomal membrane proteins: trafficking meets function.* Nature Reviews Molecular Cell Biology, 2009. **10**(9): p. 623-635.
18. Pei, J., et al., *Targeting Lysosomal Degradation Pathways: New Strategies and Techniques for Drug Discovery.* Journal of Medicinal Chemistry, 2021. **64**(7): p. 3493- 3507.
19. Osilla, E.V. and S. Sharma, *Physiology, Temperature Regulation*. 2019: StatPearls Publishing, Treasure Island (FL).
20. in *Clinical Methods: The History, Physical, and Laboratory Examinations*, rd, et al., Editors. 1990, Butterworths Butterworth Publishers, a division of Reed Publishing.: Boston.
21. Madea, B., and G. Kernbach-Wighton, *Early and Late Postmortem Changes*, in *Encyclopedia of Forensic Sciences: Second Edition*. 2013. p. 217-228.
22. Green, M.A. and J.C. Wright, *Postmortem interval estimation from body temperature data only.* Forensic Sci Int, 1985. **28**(1): p. 35-46.

23. Al-Alousi, L.M., *A study of the shape of the post-mortem cooling curve in 117 forensic cases.* Forensic Science International, 2002. **125**(2-3): p. 237-244.
24. Brown, A. and T.K. Marshall, *Body temperature as a means of estimating the time of death.* Forensic Science, 1974. **4**: p. 125-133.
25. Henßge, C. and B. Madea, *Estimation of the time since death in the early post-mortem period.* Forensic Science International, 2004. **144**(2-3): p. 167-175.
26. Gash, M. and M. Varacallo, *Physiology, Muscle Contraction.* 2019.
27. Usumoto, Y., et al., *Estimation of postmortem interval based on the spectrophotometric analysis of postmortem lividity.* Legal Medicine, 2010. **12**(1): p. 19- 22.
28. Madea, B., *Importance of supravitality in forensic medicine.* Forensic Science International, 1994. **69**(3): p. 221-241.
29. Hayman, J. and M. Oxenham, *Supravital Reactions in the Estimation of the Time Since Death (TSD)*. 2016. p. 1-12.
30. Goff, M.L., *Early postmortem changes and stages of decomposition*, in *Current Concepts in Forensic Entomology*. 2010. p. 1-24.
31. Ubelaker, D.H., *Postmortem Interval*, in *Encyclopedia of Forensic Sciences: Second Edition*. 2013. p. 24-27.
32. Myburgh, J., et al., *Estimating the postmortem interval (PMI) using accumulated degree-days (ADD) in a temperate region of South Africa.* Forensic Sci Int, 2013. **229**(1- 3): p. 165.e1-6.
33. Simmons, T., et al., *The influence of insects on decomposition rate in buried and surface remains.* Journal of Forensic Sciences, 2010. **55**(4): p. 889-892.
34. Simmons, T., R.E. Adlam, and C. Moffatt, *Debugging decomposition data - Comparative taphonomic studies and the influence of insects and carcass size on decomposition rate.* Journal of Forensic Sciences, 2010. **55**(1): p. 8-13.

35. Amendt, J., *Forensic entomology.* Forensic sciences research, 2017. **3**(1): p. 1-1.
36. Joseph, I., et al., *The use of insects in forensic investigations: An overview on the scope of forensic entomology.* Journal of forensic dental sciences, 2011. **3**(2): p. 89-91.
37. Wang, M., et al., *Forensic entomology application in China: Four case reports.* J Forensic Leg Med, 2019. **63**: p. 40-47.
38. Anderson, G.S., *Determining time of death using blow fly eggs in the early postmortem interval.* Int J Legal Med, 2004. **118**(4): p. 240-1.
39. Thyssen, P.J., et al., *Rates of development of immatures of three species of Chrysomya (Diptera: Calliphoridae) reared in different types of animal tissues: implications for estimating the postmortem interval.* Parasitology Research, 2014. **113**(9): p. 3373- 3380.
40. Patricio Macedo, M., L.C. Arantes, and R. Tidon, *Sexual size dimorphism in three species of forensically important blowflies (Diptera: Calliphoridae) and its implications for postmortem interval estimation.* Forensic Sci Int, 2018. **293**: p. 86-90.
41. Liu, R., et al., *Predicting postmortem interval based on microbial community sequences and machine learning algorithms.* Environ Microbiol, 2020.
42. Metcalf, J.L., et al., *A microbial clock provides an accurate estimate of the postmortem interval in a mouse model system.* eLife, 2013. **2013**(2).
43. Lobmaier, I.V., et al., *Bacteriological investigation--significance of time lapse after death.* Eur J Clin Microbiol Infect Dis, 2009. **28**(10): p. 1191-8.
44. Hauther, K.A., et al., *Estimating Time Since Death from Postmortem Human Gut Microbial Communities.* J Forensic Sci, 2015. **60**(5): p. 1234-40.

45. Sturner, W.Q. and G.E. Gantner, *POSTMORTEM INTERVAL - STUDY OF POTASSIUM IN*
VITREOUS HUMOR. American Journal of Clinical Pathology, 1964. **42**(2): p. 137-&.
46. Madea, B., *Is there recent progress in the estimation of the postmortem interval by means of thanatochemistry?* Forensic Science International, 2005. **151**(2-3): p. 139- 149.
47. Madea, B., et al., *References for determining the time of death by potassium in vitreous humor.* Forensic Science International, 1989. **40**(3): p. 231-243.
48. Muñoz, J.I., et al., *A new perspective in the estimation of postmortem interval (PMI) based on vitreous [K+].* Journal of Forensic Sciences, 2001. **46**(2): p. 209-214.
49. Singh, D., et al., *Linearization of the relationship between serum sodium, potassium concentration, their ratio and time since death in Chandigarh zone of north-west India.* Forensic Sci Int, 2002. **130**(1): p. 1-7.
50. Madea, B., et al., HYPOXANTHINE IN VITREOUS-HUMOR AND CEREBROSPINAL-FLUID
A MARKER OF POSTMORTEM INTERVAL AND PROLONGED (VITAL) HYPOXIA -REMARKS ALSO ON HYPOXANTHINE IN SIDS. Forensic Science International, 1994.65(1): p. 19-31.
51. Madea, B., C. Kreuser, and S. Banaschak, *Postmortem biochemical examination of synovial fluid--a preliminary study.* Forensic Sci Int, 2001. **118**(1): p. 29-35.
52. Tumram, N.K., R.V. Bardale, and A.P. Dongre, *Postmortem analysis of synovial fluid and vitreous humour for determination of death interval: A comparative study.* Forensic Science International, 2011. **204**(1-3): p. 186-190.
53. Komura, S. and S. Oshiro, *Potassium levels in the aqueous and vitreous humor after death.* Tohoku J Exp Med, 1977. **122**(1): p. 65-8.

54. Rognum, T.O., et al., *A new biochemical method for estimation of postmortem time.*
Forensic Science International, 1991. **51**(1): p. 139-146.

55. Takata, T., T. Kitao, and S. Miyaishi, *Relationship between post-mortem interval and creatine concentration in vitreous humour and cerebrospinal fluid.* Australian Journal of Forensic Sciences, 2014. **46**(2): p. 160-165.

56. Ali, R., et al., *Effect of cause of death on postmortem cerebrospinal fluid electrolytes (K+, Na+and Cl-) concentration.* Medical Forum Monthly, 2019. **30**(5): p. 69-72.

57. Sharma, P., et al., *A study of pericardial fluid enzymes activities after death and their correlation with post-mortem interval.* Journal of Indian Academy of Forensic Medicine, 2012. **34**(4): p. 346-349.

58. Swain, R., et al., *Estimation of post-mortem interval: A comparison between cerebrospinal fluid and vitreous humour chemistry.* J Forensic Leg Med, 2015. **36**: p. 144-8.

59. Madea, B. and A. Rödig, *Time of death dependent criteria in vitreous humor-Accuracy of estimating the time since death.* Forensic Science International, 2006. **164**(2-3): p. 87-92.

60. Dokgoz, H., et al., *Comparison of morphological changes in white blood cells after death and in vitro storage of blood for the estimation of postmortem interval.* Forensic Sci Int, 2001. **124**(1): p. 25-31.

61. Macedo, M.P., L.C. Arantes, and R. Tidon, *Sexual size dimorphism in three species of forensically important blowflies (Diptera: Calliphoridae) and its implications for postmortem interval estimation.* Forensic Science International, 2018. **293**: p. 86-90.

62. Cina, S.J., et al., *Flow cytometry: A screening tool for high molecular weight DNA.*
Journal of Forensic Sciences, 1994. **39**(5): p. 1168-1174.

63. Cina, S.J., *Flow cytometric evaluation of DNA degradation: A predictor of postmortem interval?* American Journal of Forensic Medicine and Pathology, 1994. **15**(4): p. 300- 302.
64. Williams, T., et al., *Evaluation of DNA degradation using flow cytometry: promising tool for postmortem interval determination.* Am J Forensic Med Pathol, 2015. **36**(2): p. 104-10.
65. Di Nunno, N., et al., *What is the best sample for determining the early postmortem period by on-the-spot flow cytometry analysis?* American Journal of Forensic Medicine and Pathology, 2002. **23**(2): p. 173-180.
66. Sampaio-Silva, F., et al., *Profiling of RNA Degradation for Estimation of Post Morterm Interval.* PLoS ONE, 2013. **8**(2).
67. Bauer, M., et al., *Quantification of mRNA degradation as possible indicator of postmortem interval--a pilot study.* Leg Med (Tokyo), 2003. **5**(4): p. 220-7.
68. Vennemann, M. and A. Koppelkamm, *Postmortem mRNA profiling II: Practical considerations.* Forensic Science International, 2010. **203**(1-3): p. 76-82.
69. Preece, P. and N.J. Cairns, *Quantifying mRNA in postmortem human brain: influence of gender, age at death, postmortem interval, brain pH, agonal state and inter-lobe mRNA variance.* Brain Res Mol Brain Res, 2003. **118**(1-2): p. 60-71.
70. Bai, X., et al., *Postmortem interval (PMI) determination by profiling of HAF mRNA degradation using RT-qPCR.* Forensic Science International: Genetics Supplement Series, 2017. **6**: p. e182-e183.

71. Ali, M.M., S.F. Ibrahim, and A.A. Fayed, *Using Skin Gene Markers for Estimating Early Postmortem Interval at Different Temperatures.* Am J Forensic Med Pathol, 2017. **38**(4): p. 323-325.

72. Eighamry, H.A., et al., *Potential use of GAPDH m-RNA in estimating PMI in brain tissue of albino rats at different environmental conditions.* Egyptian Journal of Forensic Sciences, 2017. **7**(1).

73. Candi, E., R. Schmidt, and G. Melino, *The cornified envelope: a model of cell death in the skin.* Nature Reviews Molecular Cell Biology, 2005. **6**(4): p. 328-340.

74. Koh, M.Y., B.G. Darnay, and G. Powis, *Hypoxia-associated factor, a novel E3-ubiquitin ligase, binds and ubiquitinates hypoxia-inducible factor 1alpha, leading to its oxygen-independent degradation.* Mol Cell Biol, 2008. **28**(23): p. 7081-95.

75. Bai, X.G., et al., *Postmortem interval (PMI) determination by profiling of HAF mRNA degradation using RT-qPCR.* Forensic Science International Genetics Supplement Series, 2017. **6**: p. E182-E183.

76. Kumar, S., et al., *Temperature-Dependent Postmortem Changes in Human Cardiac Troponin-T (cTnT): An Approach in Estimation of Time Since Death.* J Forensic Sci, 2016. **61 Suppl 1**: p. S241-5.

77. Gonzalez-Herrera, L., et al., *Cardiac troponin T determination by a highly sensitive assay in postmortem serum and pericardial fluid.* Forensic Sci Med Pathol, 2016. **12**(2): p. 181-8.

78. Choi, K.M., et al., *Postmortem proteomics to discover biomarkers for forensic PMI estimation.* International Journal of Legal Medicine, 2019. **133**(3): p. 899-908.

79. Pyatibratov, M.G. and A.S. Kostyukova, *Chapter five - New*

Insights into the Role of Angiogenin in Actin Polymerization, in *International Review of Cell and Molecular Biology*, K.W. Jeon, Editor. 2012, Academic Press. p. 175-198.

80. Pittner, S., et al., *Postmortem degradation of skeletal muscle proteins: a novel approach to determine the time since death.* Int J Legal Med, 2016. **130**(2): p. 421-31.

81. Izard, T. and D.T. Brown, *Mechanisms and Functions of Vinculin Interactions with Phospholipids at Cell Adhesion Sites.* J Biol Chem, 2016. **291**(6): p. 2548-55.

82. Sabucedo, A.J. and K.G. Furton, *Estimation of postmortem interval using the protein marker cardiac Troponin I.* Forensic Sci Int, 2003. **134**(1): p. 11-6.

83. Sharma, S., P. Jackson, and J. Makan, *Cardiac troponins.* Journal of clinical pathology, 2004. **57**: p. 1025-6.

84. Pittner, S., et al., *Intra- and intermuscular variations of postmortem protein degradation for PMI estimation.* International journal of legal medicine, 2020. **134**(5): p. 1775-1782.

Campell, Z.K., et al., *Talin: A potential protein biomarker in postmortem investigations.*J

Forensic Leg Med, 2016. **44**: p. 188-191.

85. Finehout, E.J., et al., *Proteomic analysis of cerebrospinal fluid changes related to postmortem interval.* Clinical Chemistry, 2006. **52**(10): p. 1906-1913.

86. Zapico, S.C., S.T. Menendez, and P. Nunez, *Cell death proteins as markers of early postmortem interval.* Cellular and Molecular Life Sciences, 2014. **71**(15): p. 2957-2962.

87. Díaz Martín, R.D., et al., *Proteomics as a new tool in forensic sciences.* Revista Espanola de Medicina Legal, 2019. **45**(3): p. 114-122.

88. Peddle, L. and G.M. Kirk, *Postmortem Organ Weights at a South African Mortuary.* Am J Forensic Med Pathol, 2017. **38**(4): p. 277-282.

89. Kitzman, D.W., et al., *Age-related changes in normal human hearts during the first 10 decades of life. Part II (Maturity): A quantitative anatomic study of 765 specimens from subjects 20 to 99 years old.* Mayo Clin Proc, 1988. **63**(2): p. 137-46.

90. Glickman, S.W., et al., *Ethical and scientific implications of the globalization of clinical research.* N Engl J Med, 2009. **360**(8): p. 816-23.

91. Fagerberg, L., et al., *Analysis of the human tissue-specific expression by genome-wide integration of transcriptomics and antibody-based proteomics.* Mol Cell Proteomics, 2014. **13**(2): p. 397-406.

92. Rajput, F.A. and R. Zeltser, *Aortic Valve Replacement*, in *StatPearls*. 2022, StatPearls Publishing Copyright © 2022, StatPearls Publishing LLC.: Treasure Island (FL).

93. Ohtsuki, I. and S. Morimoto, *Troponin*, in *Encyclopedia of Biological Chemistry (Second Edition)*, W.J. Lennarz and M.D. Lane, Editors. 2013, Academic Press: Waltham. p. 445-449.Korff, S., H.A. Katus, and E. Giannitsis, *Differential diagnosis of elevated troponins.* Heart, 2006. **92**(7): p. 987-93.

94. Schmid, J., et al., *Elevated Cardiac Troponin T in Patients with Skeletal Myopathies.* J Am Coll Cardiol, 2018. **71**(14): p. 1540-1549.

95. Gomes, A.V., et al., *Cardiac Troponin T Isoforms Affect the Ca2+Sensitivity and Inhibition of Force Development: INSIGHTS INTO THE ROLE OF TROPONIN T ISOFORMS IN THE HEART*.* Journal of Biological Chemistry, 2002. **277**(38): p. 35341-35349.

96. Hunkeler, N.M., J. Kullman, and A.M. Murphy, *Troponin I isoform expression in human heart.* 1991. **69**(5): p. 1409-1414.

97. Eltschinger, S., et al., *Eukaryotic translation elongation factor 1A (eEF1A) domain I from S. cerevisiae is required but not sufficient for inter-species complementation.* PLoS One, 2012. **7**(7): p. e42338.

98. Choi, K.M., et al., *Postmortem proteomics to discover biomarkers for forensic PMI estimation.* Int J Legal Med, 2019. **133**(3): p. 899-908.

99. Peng, X., et al., *new insights into vinculin function and regulation.* Int Rev Cell Mol Biol, 2011. **287**: p. 191-231.

100. Tomita, Y., et al., *Ultrastructural changes during in situ early postmortem autolysis in kidney, pancreas, liver, heart and skeletal muscle of rats.* Legal Medicine, 2004. **6**(1):p. 25-31.

101. Pittner, S., et al., *Postmortem degradation of skeletal muscle proteins: a novel approach to determine the time since death.* International Journal of Legal Medicine, 2016. **130**(2): p. 421-431.

102. Zissler, A., et al., *Does altered protein metabolism interfere with postmortem degradation analysis for PMI estimation?* Int J Legal Med, 2018. **132**(5): p. 1349-1356.

103. Stark, M., C.C. Kerndt, and S. Sharma, *Troponin*, in *StatPearls*. 2022, StatPearls Publishing Copyright © 2022, StatPearls Publishing LLC.: Treasure Island (FL).

104. Hoff, J., W. Wehner, and V. Nambi, *Troponin in Cardiovascular Disease Prevention: Updates and Future Direction.* Current Atherosclerosis Reports, 2016. **18**(3): p. 12.

105. Kumar, S., et al., *The effect of elapsed time on cardiac troponin-T (cTnT) degradation and its dependency on the cause of death.* Journal of Forensic and Legal Medicine, 2016. **40**: p. 16-21.

106. Di Lisa, F., et al., *Specific degradation of troponin T and I by μ-calpain and its modulation by substrate phosphorylation.* Biochemical Journal, 1995. **308**(1): p. 57-61.

107. Di Lisa, F., et al., *Specific degradation of troponin T and I by mu-calpain and its modulation by substrate phosphorylation.* Biochem J, 1995. **308 (Pt 1)**(Pt 1): p. 57-61.

108. Snape, N., et al., *The eukaryotic translation elongation factor 1A regulation of actin stress fibers is important for infectious RSV production.* Virology Journal, 2018. **15**(1): p. 182.

109. Fan, Y.-L., et al., *Mechanical Roles of F-Actin in the Differentiation of Stem Cells: A Review.* ACS Biomaterials Science & Engineering, 2019. **5**(8): p. 3788-3801.

110. Kim, J., et al., *The role of translation elongation factor eEF1A in intracellular alkalinization-induced tumor cell growth.* Laboratory Investigation, 2009. **89**(8): p. 867-874.

111. Zurawski, K.N., et al., *Examination of nocturnal blow fly (Diptera: Calliphoridae) oviposition on pig carcasses in mid-Michigan.* J Med Entomol, 2009. **46**(3): p. 671-9.Wang, X.T., K. Cheng, and L. Zhu, *[Hypoxia Accelerate β-Actin Expression through Transcriptional Activation of ACTB by Nuclear Respiratory Factor-1].* Mol Biol (Mosk), 2021. **55**(3): p. 460-467.

112. Barber, R.D., et al., *GAPDH as a housekeeping gene: analysis of GAPDH mRNA expression in a panel of 72 human tissues.* Physiol Genomics, 2005. **21**(3): p. 389-95.

113. Zainuddin, A., et al., *Effect of experimental treatment on GAPDH mRNA expression as a housekeeping gene in human diploid fibroblasts.* BMC Mol Biol, 2010. **11**: p. 59.

114. Heathfield, L.J., et al., *Ethical considerations in forensic genetics research on tissue samples collected post-mortem in Cape Town, South Africa.* BMC Med Ethics, 2017. **18**(1): p. 66.

115. Lange, N., S. Swearer, and W.Q. Sturner, *HUMAN POSTMORTEM INTERVAL ESTIMATION FROM VITREOUS POTASSIUM - AN ANALYSIS OF ORIGINAL DATA FROM DIFFERENT STUDIES*. Forensic Science International, 1994. **66**(3): p. 159-174.

Appendices

Appendix 1: Total Body Score Indicator

	Points	Description
FDS	1	1.1 No visible changes
	2	2.1 Livor mortis, rigour mortis and vibices
		2.2 Eyes: cloudy and/or tache noir
		2.3 Discoloration: brownish shades particularly at the edges. Drying of nose, ears and lips
	3	3.1 Grey to green discoloration
		3.2 Bloating of neck and face is present and/or skin blisters, skin slippage and/or marbling
		3.3 Purging of decompositional fluids out of ears, nose and mouth and/or brown to black discoloration
	4	4.1 Caving in of the flesh and tissues of eyes and throat. Skin having a leathery appearance
		4.2 Partial skeletonization, joints still together
	5	5.1 Gross skeletonization, some joints disarticulated
	6	6.1 Complete skeletonization
BDS	1	1.1 No visible changes
	2	2.1 Livor mortis, rigour mortis and vibices
	3	3.1 Grey to green discoloration
		3.2 Bloating with green discoloration and/or skin blisters, skin slippage and/or marbling
		3.3 Rectal purging of decompositional fluids
		3.4 Post-bloating: release of abdominal gasses with discoloration changing from green to black
	4	4.1 Decomposition of tissue producing sagging of flesh. Caving in of the abdominal cavity
		4.2 Skin having a leathery appearance
		4.3 Partial skeletonization, joints still together
	5	5.1 Gross skeletonization, some joints disarticulated
	6	6.1 Complete skeletonization
LDS	1	1.1 No visible changes
	2	2.1 Livor mortis, rigour mortis and vibices
		2.2 Discoloration: brownish shades particularly at the edges. Drying of fingers and toes
	3	3.1 Skin blisters and/or skin slippage and/or marbling
		3.2 Grey to green discoloration
		3.3 Brown to black discoloration
	4	4.1 Skin having a leathery appearance
		4.2 Partial skeletonization, joints and tendons still together
	5	5.1 Gross skeletonization, some joints disarticulated
	6	6.1 Complete skeletonization

Appendix 2: Formulae for Determining PMI Using Potassium and Hypoxanthine Concentrations [118]

Formulae for determining PMI (h) with $[K^+]$ (mmol/l) or [Hx] (μmol/l)

Reference	Equation obtained[a]	Formula proposed
$y = [K^+]$		
Sturner [1]	$y = 0.14x + 5.6$	$PMI = 7.14[K^+] - 39.1$
Adelson et al. [2]	$y = 0.17x + 5.36$	–
Hansson et al. [3]	$y = 0.17x + 8$	–
Coe [4]	$y = 0.332x + 4.99$ ($x < 6$ h)	–
Coe [4]	$y = 0.1625x + 6.19$ ($x \geq 6$ h)	–
Adjutantis and Coutselinis [5]	$y = 0.55x + 3.14$	–
Stephens and Richards [6]	$y = 0.238x + 6.342$	–
Madea et al. [7]	$y = 0.19x + 5.88$	$PMI = 5.26[K^+] - 30.9$
James et al. [8]	$y = 0.23x + 4.2$	$PMI = 4.32[K^+] - 18.35$
Muñoz et al. [9]	$y = 0.17x + 5.60$	$PMI = 3.92[K^+] - 19.04$
$y = [Hx]$		
Rognum et al. [10]	$y = 4.2x + 7.6$ at 5 °C $y = 5.1x + 7.6$ at 10 °C $y = 6.2x + 7.6$ at 15 °C $y = 8.8x + 7.6$ at 23 °C	
Madea et al. [11]	$y = 1.29x + 3.69$	
James et al. [8]	$y = 3.2x - 0.15$	$PMI = 0.31[Hx] + 0.05$
Our present data	$y = 3.01x + 26.45$	$PMI = 0.17[Hx] + 0.17$

[a] Variable x is postmortem (h).

Appendix 3: Recipe for 12% Resolving Gel (2 gels * 1.5mm)

dH2O	6.7ml	Final Concentrations
Tris base (PH 8.8)	5ml	1M
SDS	200ul	10%
Acrylamide	6ml	30%
APS	100ul	10%
TEMED	40ul	99%

Appendix 4: Recipe for 7% Stacking Gel (2 gels * 1.5mm)

dH2O	6.24ml	Final concentrations
Tris base (PH 6.8)	1.20ml	0.5M
SDS	50ul	10%
Acrylamide	2.38ml	30%
APS	60ul	10%
Tetramethyl ethylenediamine (TEMED)	20ul	99%

*APS and TEMED were added last and cast immediately to prevent the solidification of the gels in the beaker. These were then allowed to set 30 minutes apart with 12% prepared first before preparing the 7% which was added to top of it.

Appendix 5: 5X Loading Buffer.

1M tris (6.8)	1ml
20% SDS	2.5ml
50% Glycerol	4ml
Bromophenol blue	0.01g
*To prepare loading dye we added 25ul of B-mecarptoethanol into 75ul of loading buffer.	

Appendix 6: Towbin (Transfer Buffer)

Tris base	3.025g
Glycine	14.4g
Methanol	200ml
dH20	*added to make final volume of 1L

Appendix 7: 10xTBS(Wash Buffer)

NaCl	116.88g
Tris-Cl	60.57g
dH20	Add to 1L
*To make 1XTBS add 100ml of TBS into 1L of water. *To make TBS-T add 0.1% of Tween in 1XTSB. *To make blocking buffer we added 5g of skimmed milk into 100 ml of 1XTBS-T.	

Appendix 8: 10x Running Buffer 2L (PH 8.4)

Tris	60.6g
Glycine	288g
SDS	20g
dH20	2L
*To make 1L of 1X running buffer we added 100ml of 10X in 900ml of dH2O	

Appendix 9: Striping Buffer (PH 6.7)

B-mecarptoethanol	3.39ml
Tris base	3.79g
SDS	10g
dH20	500ml